



Australian Government



ANSTO

Science. Ingenuity. Sustainability.

LITTLE FOREST LEGACY SITE - TECHNICAL REPORT

Radionuclide Sorption Studies of Co, Cs and Sr on LFLS Soils

December 2021

M.J. Comarmond, J.J. Harrison and T.E. Payne

ANSTO E-791

ISBN 1 921268 34 4

ISSN 10307745

Purpose

The main objectives of this report are to provide:

- a summary of sorption studies of the radionuclides Cs-137, Co-57 and Sr-85 for selected soils from the Little Forest Legacy Site (LFLS).
- a compilation of soil characterisation data, sorption data and estimated distribution coefficients for Cs, Sr and Co for the selected LFLS soils.
- a comparison of the site specific Kd values with historical site data and IAEA data.
- a summary of sorption studies of Co for model mineral components of LFLS soils.

Related documents

Payne, T.E., **2012**. Background Report on the Little Forest Burial Ground Legacy Waste Site. *ANSTO/E-780*, Australian Nuclear Science and Technology Organisation.

Hankin, S. **2012**. Little Forest Burial Ground - Geology, Geophysics and Well Installation 2009–2010; *ANSTO/E-781*; Vol. 1 and Vol. 2. Australian Nuclear Science and Technology Organisation.

Payne, T.E., **2015**. Little Forest Legacy Site – Summary of Site History until the Commencement of Waste Disposal in 1960. *ANSTO E-782*. Australian Nuclear Science and Technology Organisation.

Payne, T.E., Kinsela, A.S., Bligh, M., Rowling, B., Hughes, C.E., Hankin, S., Anderson, D., Cendon, D., Wilsher, K. and Comarmond, M.J., **2018**. Installation of a Pilot Experimental Trench at the Little Forest Legacy Site. *ANSTO E-786*. Australian Nuclear Science and Technology Organisation.

Johansen, M.P., Payne, T.E., Comarmond, M.J., Harrison, J.J., Blackley, R., and Kabir, A., **2020**. Dose rate estimates to humans and wildlife for a range of potential future scenarios. *ANSTO E-787*. Australian Nuclear Science and Technology Organisation.

Scope

This document focuses on the sorption studies of Co, Cs and Sr on LFLS materials representing the various lithologies at the site.

Table of Contents

1. Introduction	3
1.1. Background.....	3
1.2. Rationale for study.....	4
2. Terminology.....	5
3. Soil sample selection and sample preparation.....	6
3.1. Sample selection	6
3.1.1. Location of sites	6
3.1.2. Sample Description.....	6
3.2. Sample preparation	7
4. Geochemical characterisation of soil samples.....	10
4.1. Characterisation methods.....	10
4.1.1. pH and EC of 1:5 slurry	10
4.1.2. Cation Exchange capacity	10
4.1.3. Elemental Assay	10
4.1.4. Grain size analysis.....	10
4.1.5. BET surface area determination	10
4.1.6. Mineralogy	10
4.2. Soil characterisation results.....	11
4.2.1. Soil pH and EC	12
4.2.2. Cation exchange capacity.....	12
4.2.3. Elemental Assays for Cs, Co and Sr inherent in samples	12
4.2.4. Grain Size and BET surface areas	13
4.2.5. Mineralogy	14
5. Sorption studies of Co, Cs and Sr onto soils	22
5.1. Radiotracers.....	22
5.2. Batch sorption method.....	22
5.3. Analysis of sorption samples	23
5.3.1. Gamma analysis	23
5.3.2. ICP analysis.....	23
5.4. Sorption results for Co, Cs and Sr	23
5.4.1. Sorption of Co, Cs and Sr for all LFLS samples.....	23
5.4.2. Sorption curves as a function of lithologies	23
5.4.3. Effect of ionic strength on sorption by CH1A samples.	27
6. Estimates of Distribution Coefficients (K_d) for Co, Cs and Sr at LFLS	29
6.1. Estimates of K_d from LFLS sorption data	29
6.1.1. K_d values for Co, Sr and Cs for LFLS materials.....	30
6.1.2. Effect of Ionic strength on K_d values for Co, Sr and Cs for CH1A soils	36
6.2. Comparison of K_d values with historical site data	38
6.3. Comparison of K_d values with IAEA data	39
6.4. Recommended K_d values for LFLS modelling	40
7. Sorption of Co on model minerals and simulated soil	42
7.1. Rationale.....	42
7.2. Materials and methods	42
7.2.1. Preparation of model soil	42
7.2.2. Characterisation of model minerals.	42
7.2.3. Methodology for sorption studies.....	42
7.3. Results and Discussion	42
7.3.1. Geochemical characterisation of model minerals and simulated soil.....	42
7.3.2. Sorption of Co on model minerals and simulated soil	43
8. Conclusions and Recommendations.....	45
9. Acknowledgements	46
10. Bibliography	47
Appendix 1: Core Logs of CH1, CH1A, CH30 and W2D	49
Appendix 2: Compilation of sorption data and K_d data for LFLS soils	55

1. Introduction

1.1. Background

The Little Forest Legacy Site (LFLS) is located within the ANSTO Buffer Zone Boundary near Sydney in South Eastern Australia. This site, previously known as the Little Forest Burial Ground (LFBG), was used by the former Australian Atomic Energy Commission (AAEC) during the 1960's to dispose of waste containing low levels of radioactivity in a series of shallow trenches which was the accepted international practice at the time [Payne, 2012]. Figure 1.1 shows the location of Little Forest Legacy Site (LFLS) in relation to Australia and the city of Sydney (inset), the ANSTO Buffer Zone boundary, the location of the waste disposal trenches and the local topography. Historically, a number of drilling operations took place at the site since 1958 resulting in monitoring boreholes/wells at the site. There has been regular environmental monitoring of the site since 1966, during which measurable amounts of various radionuclides including Co-60, Sr-90 and Cs-137 have been observed in some soils, groundwater and vegetation samples taken in close proximity to the disposal area [Payne 2012, AAEC 1985].

A comprehensive soil sampling campaign was undertaken in 2009 as part of a research program encompassing field and laboratory studies of the LFLS. Around this time, 33 soil cores (coded CH series) were collected with depths below the ground surface ranging between 1.7 and 5.0 m and drilled using push tube and sectional flight auger (SFA) methods [Hankin, 2012]. The direct push method yielded intact soil cores while the auger technique yielded unconsolidated soil auger chips. These cores were used to provide lithological information and samples for laboratory testwork. A further drilling program was undertaken in 2010 to install additional wells, categorised as the W series [Hankin, 2012].

Geochemical characterisation and sorption studies performed on subsamples from the CH and W series are the subject of this report.

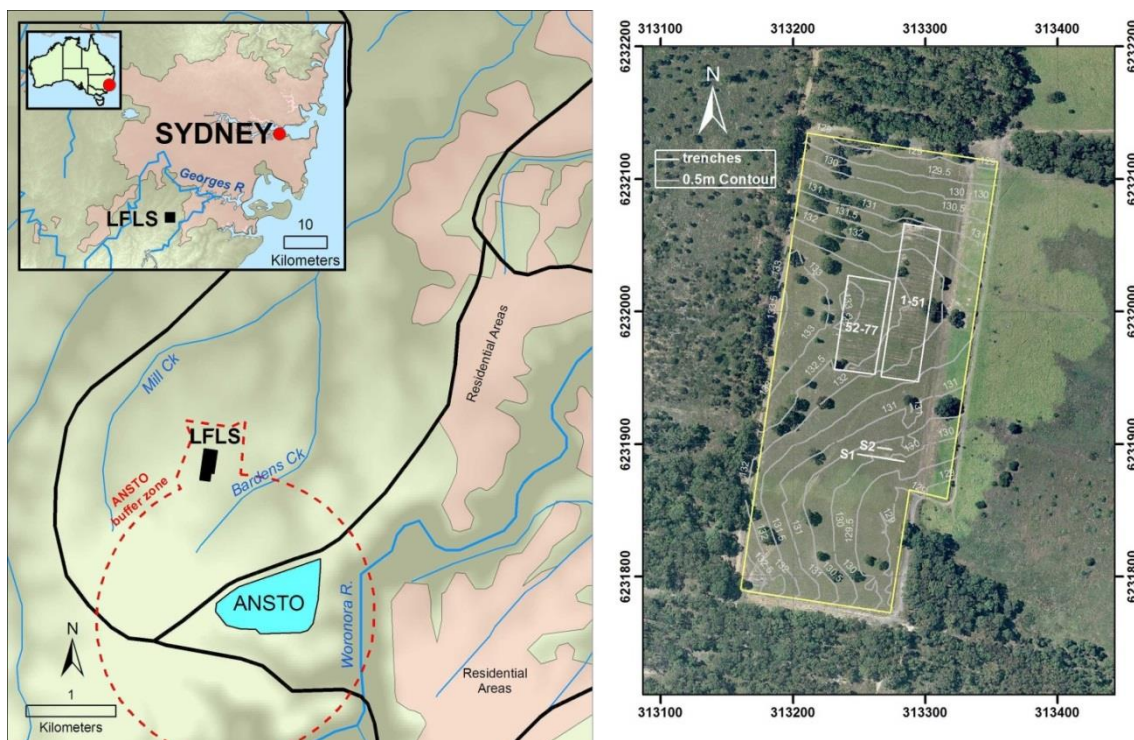


Figure 1.1: Location of Little Forest Legacy Site (LFLS) in relation to Australia and the city of Sydney and ANSTO (inset). The schematic on the left indicates the ANSTO buffer zone (red dashed line) which includes the LFLS and the photograph on the right is of the LFLS site showing the location of the waste disposal trenches (labelled 1-51, 52-77, S1 and S2) and the local topography [Cendon et al., 2015].

1.2. Rationale for study

The purpose of the present study was to investigate the sorption of the radionuclides Co, Cs and Sr on soil materials sourced from cores sampled at the Little Forest Legacy site. Co, Sr and Cs were chosen as elements of interest because waste containing radioactive isotopes of these elements (primarily Co-60, Sr-90 and Cs-137) are known to have been disposed at this site and are (or have previously been) readily detectable in some environmental samples collected from the site (e.g. groundwater, soils and vegetation). The soil samples were taken at various depth intervals along the core length representing the various lithologies at the site. The sorption studies, coupled with targeted characterization of the samples, will provide insight to the key site characteristics governing contaminant release and transport of these radionuclides at Little Forest. The sorption studies allow for an estimate of site specific distribution coefficient (K_d) values for Co, Sr and Cs under controlled experimental conditions that could be utilised in groundwater fate and transport modelling and dose assessment studies.

2. Terminology

AAEC	Australian Atomic Energy Commission
ANSTO	Australian Nuclear Science and Technology Organisation
CEC	Cation Exchange Capacity
CH	Corehole
CSIRO	Commonwealth Scientific Industry Research Organisation
EC	Electrical Conductivity
IAEA	International Atomic Energy Agency
ICPAES	Inductively Coupled Plasma Atomic Emission Spectrometry
ICPMS	Inductively Coupled Plasma Mass Spectrometry
Kd	Distribution Coefficient
LFBG	Little Forest Burial Ground
LFLS	Little Forest Legacy Site
OM	Organic Matter
SFA	Sectional flight auger
XRD	X-ray Diffraction

3. Soil sample selection and sample preparation

3.1. Sample selection

3.1.1. Location of sites

The samples for sorption studies presented in this report were surface soils and corehole samples obtained from CH1, CH1A, CH30 and W2D site locations indicated in Figure 3.1. These sites represent various locations in the vicinity and well away from the legacy trenches with CH1 and CH1A located at the base and midway between the two sets of legacy trenches and CH30 located further north and near the only trench water sampler in existence at the site of the legacy trenches [Payne, 2013] at this point in time. W2D was located at the south western end of the LFLS, far removed from the legacy trenches. It was noted that materials from this location are likely to be impacted by discharge from the nearby Harrington's Quarry due to groundwater flow paths [Cendon et al., 2015].

3.1.2. Sample Description

The samples selected for the testwork are summarised in Table 3.1.

Table 3.1 Samples for characterisation and sorption studies in the vicinity of the trenches.

	CH1	CH1A	CH30
LITHOLOGY	Depth (m)		
TOPSOIL	0 - 0.2		0 - 0.2
SILTY CLAY			0.2 - 0.4
CLAY		0.4 - 0.6	0.4 - 1.0
SHALEY CLAY		1.4 - 1.6	1.0 - 1.5
SILTSTONE			1.5 - 2.0
SHALE		2.4 - 2.6	
		3.4 - 3.6	

Table 3.2 Background samples for characterisation and sorption studies.

	W2D
LITHOLOGY	Depth (m)
TOPSOIL	0 - 0.5
SILTY CLAY	1.0 - 1.5
SHALE	2.5 - 3.0
CLAY	4.5 - 5.0
SILTSTONE	6.5
SHALE	9.5

These samples represent the stratigraphy at the LFLS site, classified into lithological units as described in core logs, namely topsoil, leached/weathered zone shale (further classified as silty clay, clay, shaley clay and siltstone) and parent shale. Figure 3.2 shows a schematic and photograph of CH1A as an example of a typical corehole profile. The core logs for CH1, CH1A, CH30 and W2D are provided in Appendix 1.

3.2. Sample preparation

A description of the coring and subsampling of the various cores is provided below. There was some variation in the methods used for subsampling of the various surface soils and cores because of the limited amount of sample available from the drilling programs.

CH1A: The core was acquired by a direct push method. The soil core was split in half lengthways and four 20 cm slices were subsampled from the core as indicated by the arrows in Figure 3.2 to represent the following lithologies:

- Between 0.4 and 0.6 m – clay
- Between 1.4 and 1.6 m – shaley clay/shale
- Between 2.4 and 2.6 m – shale
- Between 3.4 and 3.6 m – shale

CH30: The first two metres of core below the ground surface was obtained using a direct push method. The entire length of this core was subsampled in 10 cm intervals.

W2D: Samples were obtained from grab samples previously collected during the field augering for well construction. Additional sub-samples of bulk material were used for the mineralogical assessment. (see Table 4.2)

CH1 surface soil: The sample was obtained by direct push method.

All samples were air-dried and disaggregated using a rubber mallet and a sub-sample taken for grain size analysis. The remainder was oven dried at 60 °C prior to sample processing. Coning and quartering and/or a sample riffler were used to provide representative samples with size fractionation (< 2 mm; < 1 mm) facilitated by sieving to be used for sorption and soil characterisation studies. Pulverised sub-samples were prepared using a ring-grinder to be used for elemental assays. All samples were retained in tared plastic sealable bags and stored at ambient temperature.

LFBG - Wells and Coreholes

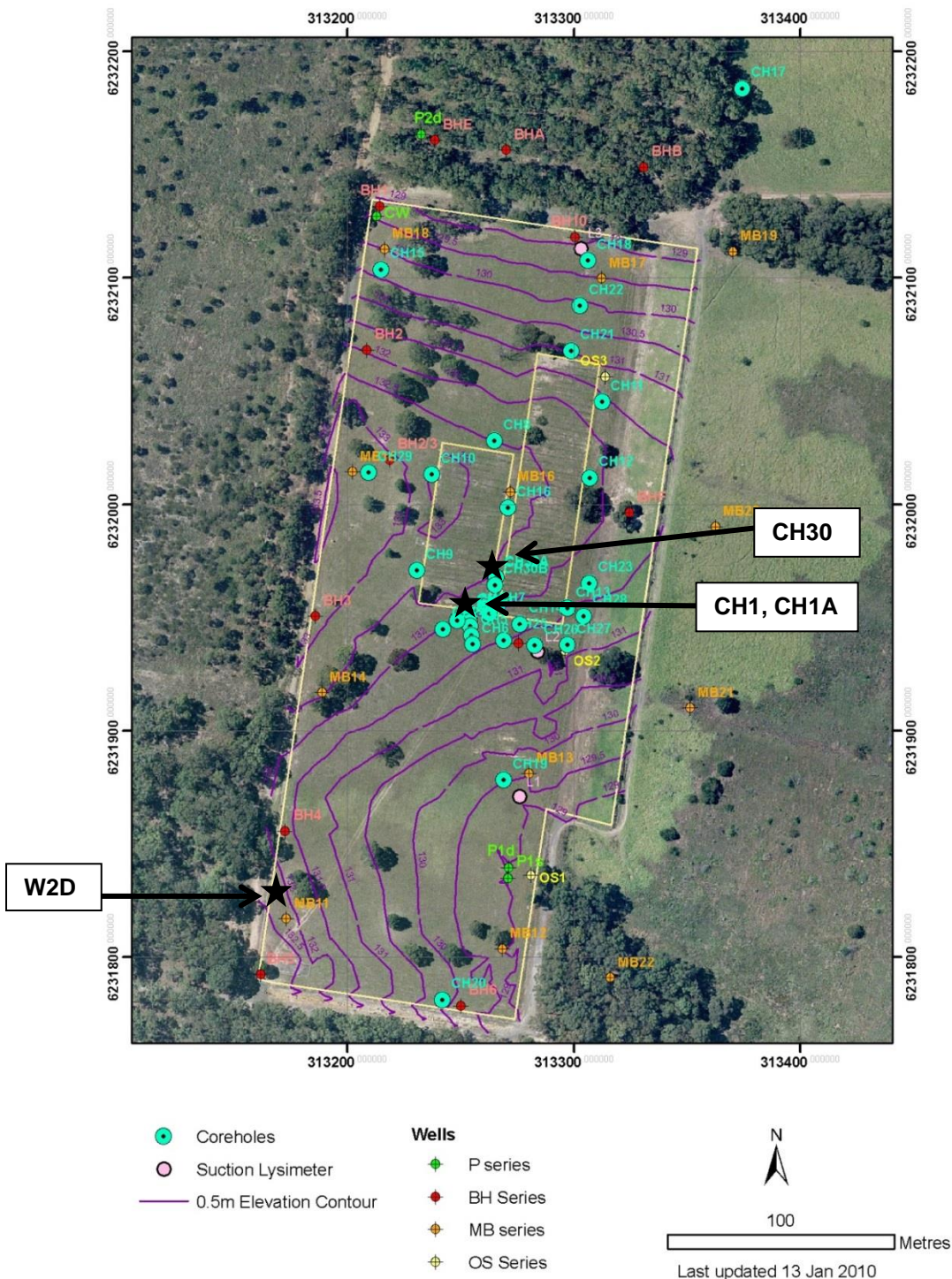


Figure 3.1: Location of Little Forest Legacy Site (LFLS) samples used for soil characterisation and sorption studies.

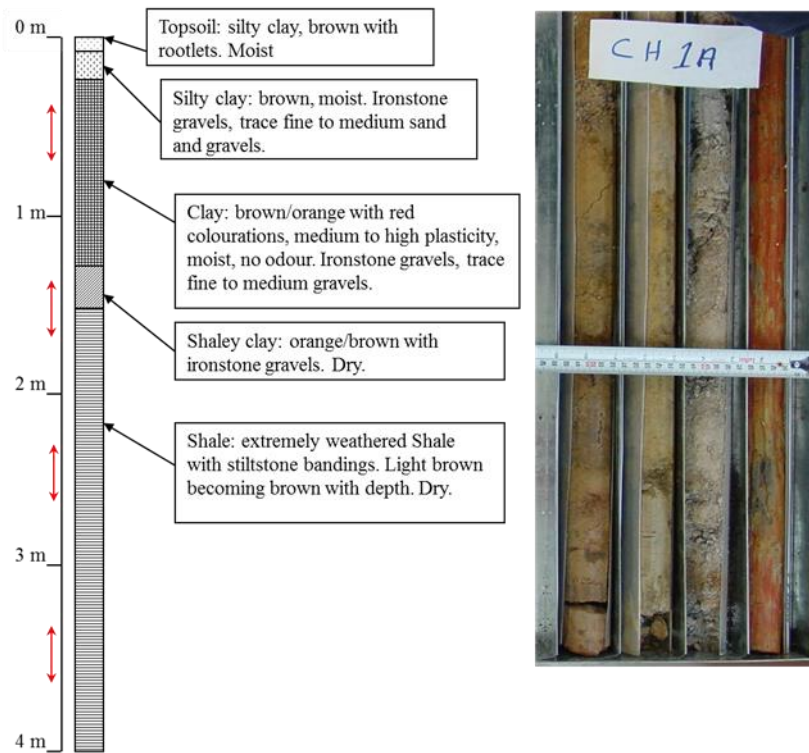


Fig. 3.2: Schematic of the various lithologies for CH1A and a photograph of the CH1A cores. The core was partitioned in 1 m intervals, with the core at the far right of the photograph representing a subsection of core obtained from the 0 – 1 m depth, and the core at the far left of the photograph representing a subsection from the 3 – 4 m depth.

4. Geochemical characterisation of soil samples

4.1. Characterisation methods

4.1.1. pH and EC of 1:5 slurry

The pH and electrical conductivity of soil samples (EC) were conducted on a 1:5 soil/water extract as per the method of Rayment and Higginson [1992]. Non-pulverised samples (5 g) were prepared as slurries and placed in a shaker bath or incubator (150 rpm, at 25 °C) for one hour. The samples were allowed to settle for 25 minutes prior to measurements of EC and pH, respectively.

4.1.2. Cation Exchange capacity

The cation exchange capacities (CEC) of non-pulverised samples were determined using methylene blue and the tetrasodium pyrophosphate method of Wang *et al.* [1996]. Half a gram of soil sample was accurately weighed into a conical flask to which 50 mL of a 20 g/L sodium pyrophosphate solution was added. The slurry was gently boiled on a hot plate for ca. 20 minutes and then allowed to cool at room temperature. The suspension was titrated with a fresh solution of methylene blue (0.05 M or 0.1 M) with 0.5 mL aliquots, using the spot test to determine the end point.

4.1.3. Elemental Assay

Elemental assays were conducted on pulverised sub-samples that were subsequently microwave digested in strong acid and analysed by inductively coupled plasma atomic emission spectroscopy (ICP-AES) and inductively coupled plasma mass spectrometry (ICP-MS). The subsamples were digested according to ANSTO method I-2995 - Inorganic: microwave assisted acid digestion and analysed using ANSTO method I-2809 (ICPMS) and ANSTO method I-3775 (ICPAES).

4.1.4. Grain size analysis

Two methods were used for grain size analysis. The grain size determinations for the CH1, CH30 and W2D samples were performed using a Mastersizer 2000 [Malvern Instruments Ltd., 2007]. This method is performed for size fractions < 1 mm and provides classification of grain size as sand, silt and clay. Samples were sieved to < 1 mm and the sieved subsamples were initially dispersed in water and ultrasonicated for several minutes prior to analysis on the Mastersizer 2000. The analyses for the CH1A samples were performed by CSIRO [Raven and Self, 2011], with a focus on an assessment of the finer clay fractions. The method used involved repeated dispersion of the bulk sample in 1 M sodium chloride solution followed by centrifugation to recover the coarse clay (> 2 µm) and fine clay (< 2 µm) fractions.

4.1.5. BET surface area determination

The specific surface area was determined using the BET-N₂ gas adsorption method [IUPAC, 1985] with samples degassed under vacuum at a temperature of 100 °C prior to the BET surface area determination.

4.1.6. Mineralogy

The mineralogical assessment of CH1, CH30 and W2D samples was conducted at ANSTO. Samples were milled in a ring grinder and analysed as pressed powders with random orientation. The powder X-ray diffraction data were obtained with an X'pert Pro diffractometer using Cu K_{α1,2} radiation with a Ni filter. The PANalytical analysis package High Score Pro was used for quantitative analysis

The mineralogical assessment of the CH1A samples was performed by CSIRO [Raven and Self, 2011]. Subsamples were micronized for 10 min under ethanol and the resulting slurries oven dried at 60 °C. These samples were subsequently homogenised in a mortar and pestle and prepared as pressed powders for XRD. The samples showed variable hydration of the interlayer, so were calcium saturated and the data reanalysed.

To recover the < 2 µm and > 2 µm fractions, a subsample of the bulk was prepared by repeated dispersion of the sample in 1 M NaCl as described in Section 4.1.4. The suspensions were flocculated with excess NaCl, treated with acetic acid to remove carbonate minerals, calcium saturated twice (using 1 M CaCl₂), washed with water followed by alcohol, with centrifugation at each step. The samples were oven dried at 60 °C and ground in an agate mortar and pestle and prepared as pressed powders to achieve random orientation of the particles for XRD analysis [Raven and Self, 2011]. The process was also repeated for XRD analysis of the < 0.2 µm and > 0.2 µm sub-samples (randomly oriented).

Oriented specimens of the < 2 µm and < 0.2 µm fraction were prepared by dispersion of the coarse clay and fine clay fractions in deionised water using a high energy ultrasonic probe, and deposition onto 0.2 µm cellulose nitrate filter membranes under suction. The sample was subsequently magnesium saturated using 1 M MgCl₂, washed several times with deionised water followed by glycerol and mounted onto a 25 mm aluminium disc using double sided tape.

The XRD patterns were recorded with a PANalytical X'pert Pro Multi-purpose Diffractometer using Fe filtered Co K_α radiation. Quantitative analysis was performed on the XRD data using the commercial package SIROQUANT from Sietronics Ltd and results normalised to 100%.

4.2. Soil characterisation results

The geochemical characterisation data obtained for the various subsamples are summarised in Table 4.1.

Table 4.1 Summary of soil physical and chemical properties

COREHOLE	Depth interval (m)	Lithology	size fraction	pH	EC (µS/cm)	CEC (cmol/kg)	BET SA (m ² /g)	Elemental Assay		
								Cs (µg/kg)	Co (µg/kg)	Sr (mg/kg)
CH1	0 - 0.2	topsoil	< 2 mm	5.48	37.0	nd	20.0	nd	nd	nd
CH1A	0.4 - 0.6	clay	< 1 mm	5.33	11.1	16.3	40.2	14 000	2 030	164
	1.4 - 1.6	shaley clay	< 1 mm	5.14	13.7	17.3	47.1	17 000	1 090	242
	2.4 - 2.6	shale	< 1 mm	5.45	8.1	7.0	36.2	14 600	1 330	206
	3.4 - 3.6	shale	< 1 mm	5.91	13.0	10.1	27.2	13 700	4 610	170
CH30	0 - 0.2	topsoil	< 2 mm	5.06	16.6	7.8	18.3	10460	2300	136
	0.2 - 0.4	silty clay	< 2 mm	5.53	22.1	9.3	15.1	9360	2740	81.5
	0.4 - 0.6	clay	< 2 mm	5.50	21.7	14.6	20.6	12400	226	145
	0.6 - 0.8	clay	< 2 mm	5.03	18.1	16.3	45.2	13600	1420	191
	0.8 - 1.0	clay	< 2 mm	5.27	13.3	15.2	38	11000	1310	142
	1.0 - 1.2	shaley clay	< 2 mm	5.25	12.1	5.6	24.1	11300	3900	200
	1.2 - 1.4	shaley clay	< 2 mm	5.07	11.0	4.0	23	10450	1685	179
	1.4 - 1.6	shaley clay/siltstone	< 2 mm	5.74	8.5	3.6	25.8	12000	895	192
	1.6 - 1.8	siltstone	< 2 mm	5.56	8.1	7.8	25.5	11500	11400	184
1.8 - 2.0	siltstone	< 2 mm	5.29	10.7	10.0	25.8	11350	11125	192	
W2D	0 - 0.5	topsoil	< 2 mm	5.44	24.1	nd	71.9	nd	nd	nd
	1.0 - 1.5	silty clay	< 2 mm	4.84	25.9	11.1	45.5	7860	1950	98.4
	2.5 - 3.0	shale	< 2 mm	5.21	23.0	7.2	32.4	6750	2800	167
	4.5 - 5.0	clay	< 2 mm	5.27	34.8	6.9	14.6	5290	5420	214
	6.5	siltstone	< 2 mm	6.83	41.2	3.9	9.1	1670	15700	125
	9.5	shale	< 2 mm	6.88	50.9	5.5	11.3	32700	23600	288

nd = not determined

4.2.1. Soil pH and EC

The pH of the soils for core depths up to 5 m typically ranges from 4.9 to 5.9. The deeper samples of W2D (depth greater than 5 m) are near neutral (soil pH 6.6 to 6.8) and this is attributed to the elevated siderite content in those samples as determined from mineralogical assessment (see Section 4.2.5 below).

The W2D samples have higher electrical conductivities (EC) ranging from 23 to 51 $\mu\text{S}/\text{cm}$ in comparison with the CH1A and CH30 samples. The EC for subsamples of the CH1A and CH30 cores are similar along the core profile, ranging from 8 to 22 $\mu\text{S}/\text{cm}$. The EC for W2D samples typically increase with depth and the elevated values may arise from the impact of leachate flow from the nearby Harrington's Quarry [Cendon et al., 2015] as well as from the dissolution of carbonates inherent in these materials.

4.2.2. Cation exchange capacity

The cation exchange capacities (CEC) for CH1A, CH30 and W2D soils are reported in Table 4.1 and range from 7.0 to 17.3 cmol kg^{-1} for the CH1A samples, 3.6 to 16.3 cmol kg^{-1} for the CH30 samples, and 3.9 to 11.1 cmol kg^{-1} for the W2D samples. CECs determined for soil samples from LFLS have previously been reported with values ranging from 7.1 to 9.0 cmol kg^{-1} as shown in Table 4.2 [Isaac and Mears, 1977]. The four soils from the earlier study contained more than 50% kaolinite and have low CEC values. This is consistent with kaolinitic soils where kaolinite as the dominant clay has a low ability to exchange ions [Goldberg et al., 2005].

Table 4.2: Description and cation exchange capacity of a soil profile at LFLS (reproduced from Isaac and Mears, 1977).

Fraction	Sampling depth (m)	Description	Composition	CEC (cmol kg^{-1})
F1	0.0-0.5	topsoil	Kaolinite (>50%) Mica, smectite Quartz (<50%)	7.3
F2	0.5-1.0	Red-brown clay	Kaolinite (80%) Mixed-layer mica –smectite, Quartz (20%)	9.0
F3	1.0-1.5	Greyish clay	Kaolinite (80%) Mixed-layer mica- smectite, Quartz (20%)	7.1
F4	1.5-2.5	Weathered shale	Kaolinite (65%) Micaceous clay mineral (35%)	8.3

4.2.3. Elemental Assays for Cs, Co and Sr inherent in samples

Results of the chemical assays for Cs, Co and Sr inherent in the various subsamples are summarized in Table 4.1. With the exception of the W2D shale material sourced at ca 9.5 m below the ground surface, the samples of CH1A and CH30 are more elevated in inherent Cs content than the W2D samples. The Cs content in these samples range from 9.3 ppm to 17 ppm and are significantly higher than the average crustal abundance value of 2 ppm and the global average shale value for Cs of 7 ppm [Krauskopf, 1983; Rudnick and Gao, 2014] whereas the inherent Cs for the W2D samples ranges from 1.6 to 7.9 ppm.

The inherent Co in the samples ranges from 230 to 23 600 ppb, with the majority of samples well below both the average crustal abundance of 26 600 ppb and the global average shale value of 20 000 ppb. The siltstone samples from CH30 and the siltstone and shale samples from W2D have significantly higher Co content (> 10 000 ppb) with the W2D shale sample below 9.5 m exceeding the global average shale value.

The inherent Sr in the samples ranges from 82 to 290 ppm. These values fall well below the average crustal abundance for Sr (320 ppm) and the global average shale value for Sr (400 ppm).

4.2.4. Grain Size and BET surface areas

The grain size distribution for subsamples of CH30 is shown in Figure 4.1. Sieving established that up to ca 30% of the particles are > 1 mm when fractionating samples with a maximum particle size of 2 mm. The clay and silt fraction were found to be highest for the first meter below the ground surface, followed by a decrease in clay fraction below 1 m. For grain size analysis of the < 1 mm fraction using the Mastersizer, fluctuating results were obtained on replicate sub-samples when using different ultrasonication times, suggestive that water may not have been the best dispersant for clays and/or that ultrasonication was not suitable for disaggregating clay fractions. These aspects were not explored further in the present study.

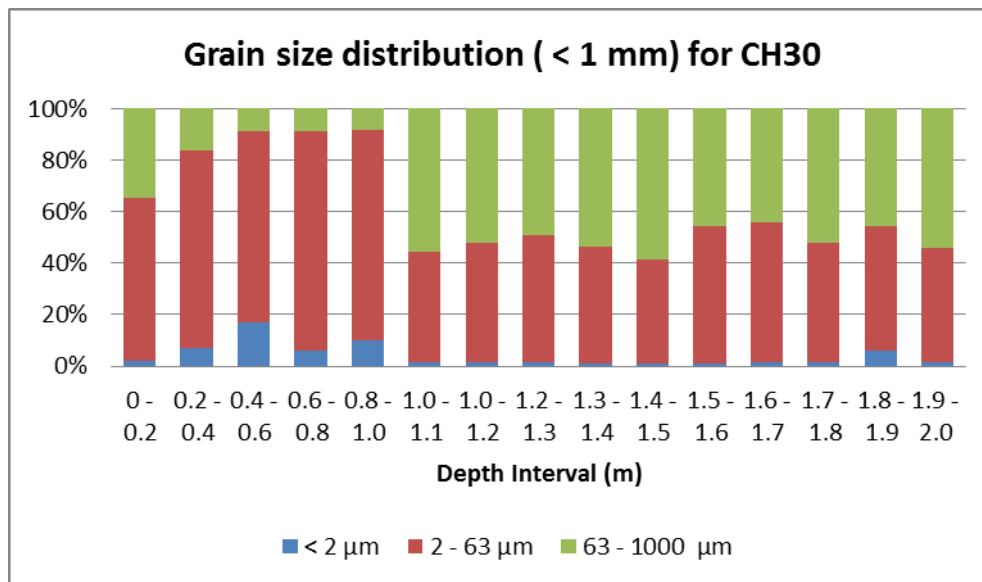


Fig. 4.1: Grain size distribution for CH30 (< 2 mm).

The grain size distribution for CH1A was performed by CSIRO using a different method, with greater emphasis on the distribution of coarse (< 2 μm) and fine clay (< 0.2 μm) fractions. Figure 4.2 shows that both the coarse and fine clay fractions, respectively, decrease with depth for the core profile. The clay lithology sample (0.4 – 0.6 m) had significantly more coarse and fine fraction clay (< 2 μm) compared to the shaley clay and shale samples. There is also a decrease in fine fraction clay with depth.

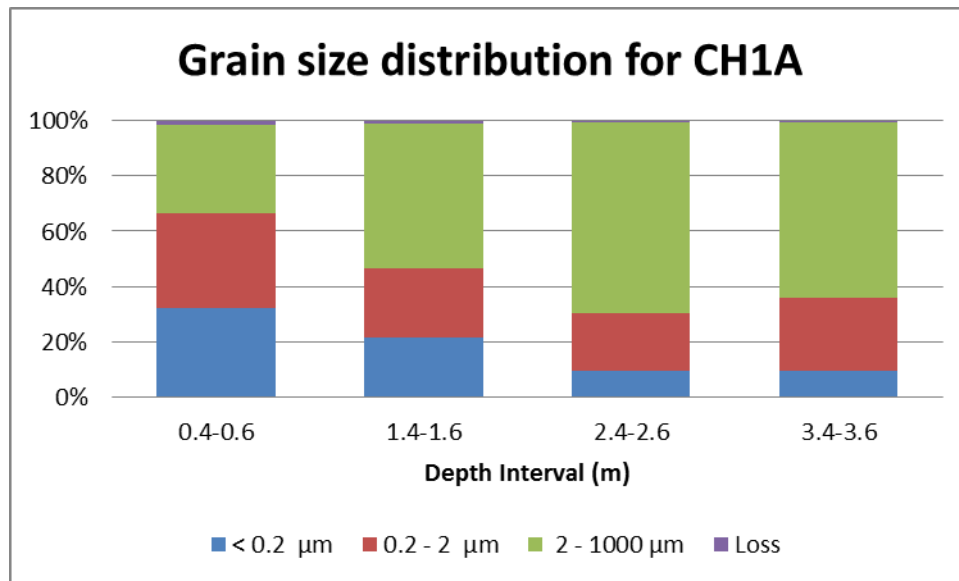


Fig 4.2: Distribution of grain size in bulk samples (< 1 mm). The coarse clay fraction is represented by the 0.2 – 2 μm fraction, while the fine clay fraction is the fraction below 0.2 μm.

The BET surface areas for samples of CH1A range between 27 and 47 m²/g while the BET surface areas for the CH1 topsoil in the near vicinity was somewhat lower at 20 m²/g. The BET surface areas for the CH30 samples range from 15 to 45 m²/g. The BET surface area for samples of W2D range from 9.1 to 72 m²/g with the highest BET observed for the topsoil sample.

4.2.5. Mineralogy

A summary of the mineralogical assessment of the samples is given in Table 4.3 with the distribution of minerals in each sample shown in Figures 4.3 – 4.12.

The CH1 sample is a topsoil/fill with ca. 63% quartz and 34% clay and mica minerals (predominantly kaolinite and mixed layer clays) with trace amounts of anatase, rutile and goethite (each < 1%) (Figures 4.3 and 4.4).

The CH1A samples comprise predominantly of quartz (25-31%), interstratified illite-smectite (23-35%) and kaolinite (28-31%) of similar proportions, with ca. 6-11% mica and/or illite. The interstratified illite-smectite has been estimated to be composed of approximately 70% illite and 30% smectite layers. Smectite (4-8%) was also found in the uppermost clay layers [Raven and Self, 2011]. Trace anatase and iron oxides were found in the majority of samples. XRD analysis of the < 1 mm, < 2 μm and < 0.2 μm fractions of the CH1A soils (Figs. 4.4 to 4.6) show that kaolin and interstratified illite-smectite and smectite occur predominantly in the finest clay fractions.

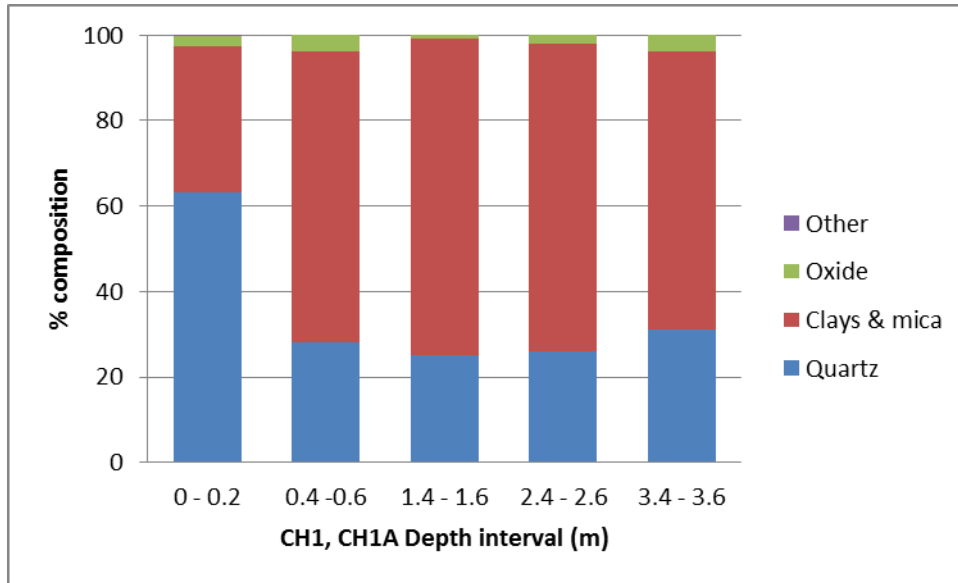


Figure 4.3: Percentage composition of quartz, clays & mica and oxides in corehole samples of CH1 and CH1A for various depth intervals.

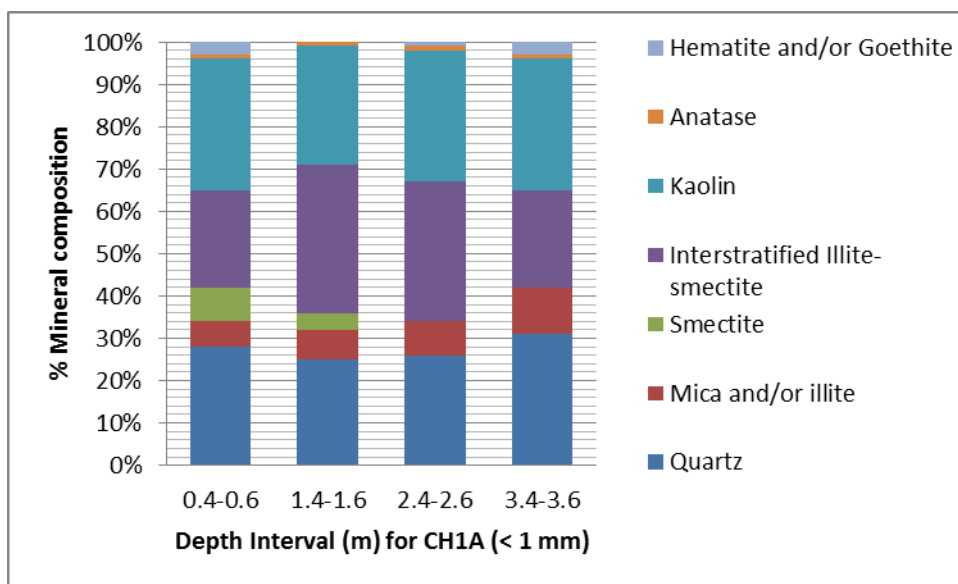


Figure 4.4: Mineralogical composition of the < 1 mm fraction of CH1A corehole samples at various depth intervals as determined by XRD analysis.

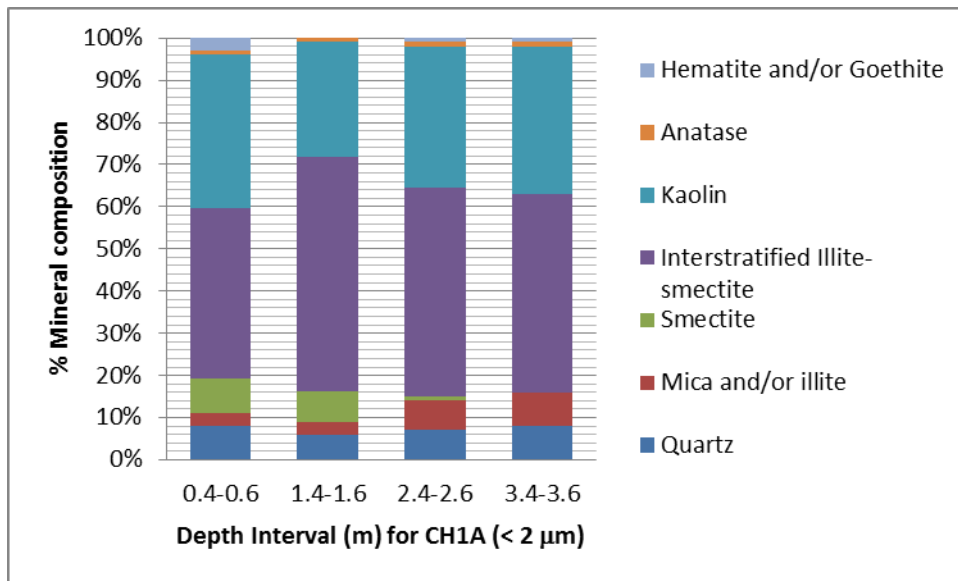


Figure 4.5: Mineralogical composition of the < 2 μm fraction of CH1A corehole samples at various depth intervals as determined by XRD analysis.

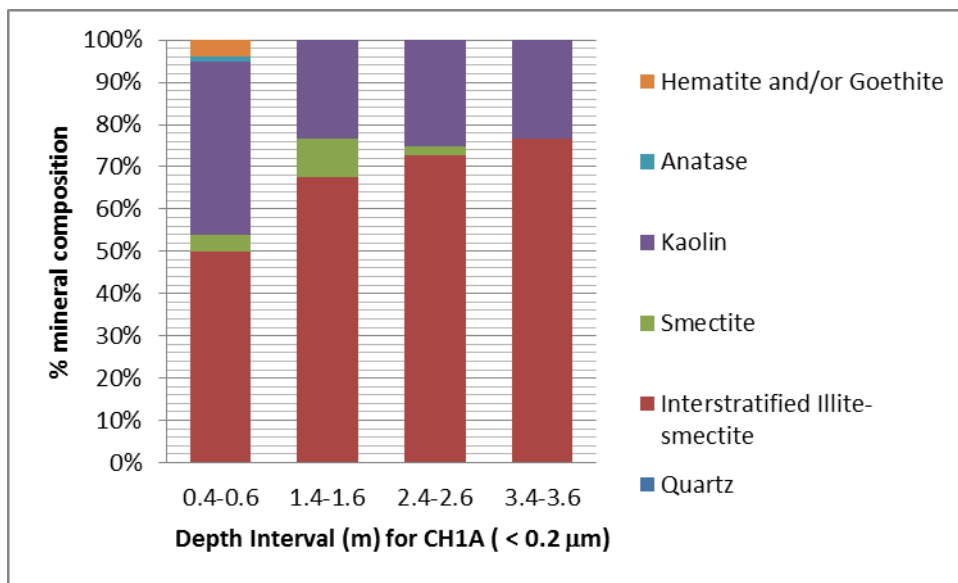


Figure 4.6: Mineralogical composition of the < 0.2 μm fraction of CH1A corehole samples at various depth intervals as determined by XRD analysis.

Figure 4.7 and 4.8 show the distribution for quartz, clays and mica, and oxides for the < 2 mm and < 1 mm samples of CH30, respectively. The mineralogical distribution is similar for sub-samples at the two particle size fractions for these mineral groups. The CH30 samples are higher in quartz content (40 – 60%) relative to the CH1A samples, with clays and mica making up the bulk of the difference. These samples also have oxide content of up to ca. 10%, with both anatase and goethite pervasive throughout the 2 m depth profile. The mineralogical composition for the CH30 samples is shown in Figures 4.9 and 4.10.

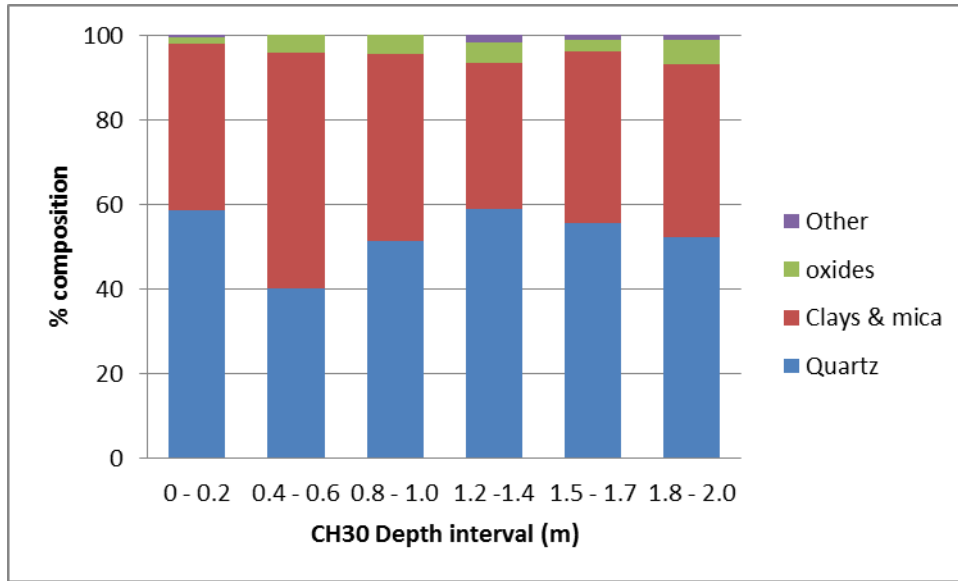


Figure 4.7: Percentage composition of quartz, clays & mica and oxides in corehole samples of CH30 (< 2 mm) for various depth intervals.

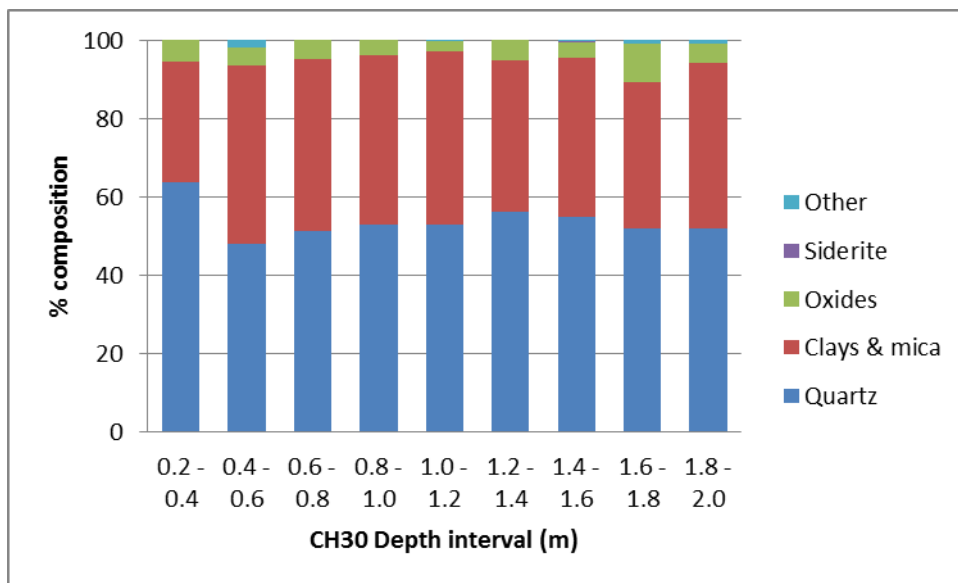


Figure 4.8: Percentage composition of quartz, clays & mica and oxides in corehole samples of CH30 (< 1 mm) for various depth intervals.

Table 4.3: Mineralogical assessment of LFLS soil samples from coreholes CH1, CH1A, CH30 and W2D.

COREHOLE	Lithology	Depth interval (m)	Mid-point (m)	size fraction	TECTOSILICATES		PHYLOSILICATES						OXIDES/HYDROXIDES				CARBONATES	
					Quartz & Feldspars (%)		Clay & Mica minerals (%)						Ti oxides (%)		Fe oxide/hydroxides (%)		(%)	
					Qtz	Orthoclase	Kaolin	Dickite	Mixed Layer	Illite	Smectite	Mica and/or illite	Muscovite	Biotite	Rutile	Anatase	Goethite	Hematite
CH1	topsoil	0-0.2	0.1	<2 mm	63.1		17.3	1.7	15					0.2	0.8	0.7	0.9	
CH1A	clay	0.4-0.6	0.5	<1 mm	28		31		23		8	6				1	3	
	shaley clay	1.4-1.6	1.5	<1 mm	25		28		35		4	7				1		
	shale	2.4-2.6	2.5	<1 mm	26		31		33			8				1	1	
	shale	3.4-3.6	3.5	<1 mm	31		31		23			11				1	3	
CH30	topsoil	0-0.2	0.1	<2 mm	58.6	0.4	23.7	8.1	7.3					0.2	0.3	1.3	0	0
				<1 mm	58.4	0.2	17.2	9.1	9.5					1.2	0.9	1.4	2	0.3
	silty clay	0.2-0.4	0.3	<1 mm	63.8	0.2	6.1	5.8	18.4					0.4	1.6	1.3	1.1	1.5
	clay			<2 mm	40	0	12.2	6.1	37.5					0	0	0.8	3.3	0
	clay	0.4-0.6	0.5	<1 mm	47.9	0.2	11.9	4.2	29.4					0	0.2	1.3	3.3	
	clay	0.6-0.8	0.7	<1 mm	51.1	0	10.9	10.7	22					0.3	0	1.3	3	0.6
	clay			<2 mm	51.4	0	27.6	7	9.4					0.1	0	1.5	2.4	0.5
	clay	0.8-1.0	0.9	<1 mm	52.8	0	20.8	6.9	15.4					0.2	0.1	1.6	2	0.2
	shaley clay	1.0-1.2	1.1	<1 mm	52.8	0.1	15.7	4.4	23.8					0.3	0	1.1	1.4	0.2
	shaley clay			<2 mm	58.9	2	19.6	6.6	7.6					0.7	0.4	1.6	2.7	0
	shaley clay	1.2-1.4	1.3	<1 mm	56.2	0	17.6	5.2	15.4					0.4	0.3	1.3	2.7	0.9
	shaley clay/siltstone	1.4-1.6	1.5	<1 mm	54.9	0.2	16.7	6.8	16.5					0.5	0.2	1	2.1	0.8
	siltstone	1.5-1.7	1.6	<2 mm	55.7	1.3	20	5	14.8					0.6	0	1.2	1.4	0
	siltstone	1.6-1.8	1.7	<1 mm	51.9	1.9	8.1	10.3	17.9					1.1	0.7	1.1	6	1.8
siltstone			<2 mm	52.3	1.1	19.5	5.5	15.2					0.5	0.4	1.5	3.3	0.6	
siltstone	1.8-2.0	1.9	<1 mm	52	0.3	18.2	5.2	18.4					0.3	0	1.2	3.6	0	
W2D	topsoil	0-0.5	0.25	<2 mm	29.1		33.4	1.8	1.3						1.8	32.6		
	silty clay	0.5-1.0	0.75	bulk	28.9		38.6	11.4		4				1	2.1	10.6		1.1
	shaley clay	2.0-2.5	2.25	bulk	55.1		25.6	2.5		4.6		2.4		0.7	0.8	1.7		0.6
	shaley clay	4.0-4.5	4.25	bulk	57.9		24.3	3		3.3		8.5		0.5	0.4	4.3		0.1
	clay	4.5-5.0	4.75	bulk	61		21.7	1.8		4.5		7.6		0.4	0.7	2.3		0.2
	siltstone	6	6	bulk	68.1		11.9	4.9		2.1		4.7		0.5	0.2	1		6.6
	siltstone	7.5	7.5	bulk	72.2		11.4	4.4		2.3		3.9		0.3	0.2	0.4		4.8
	shale	10	10	bulk	51.7		15.2	2.9		5.7		6.9		0.3	1.1	0.5		15.8
	shale	10.5	10.5	bulk	58.1		15.4	3.3		4.1		6.3		0.2	0.8	1.1		10.9

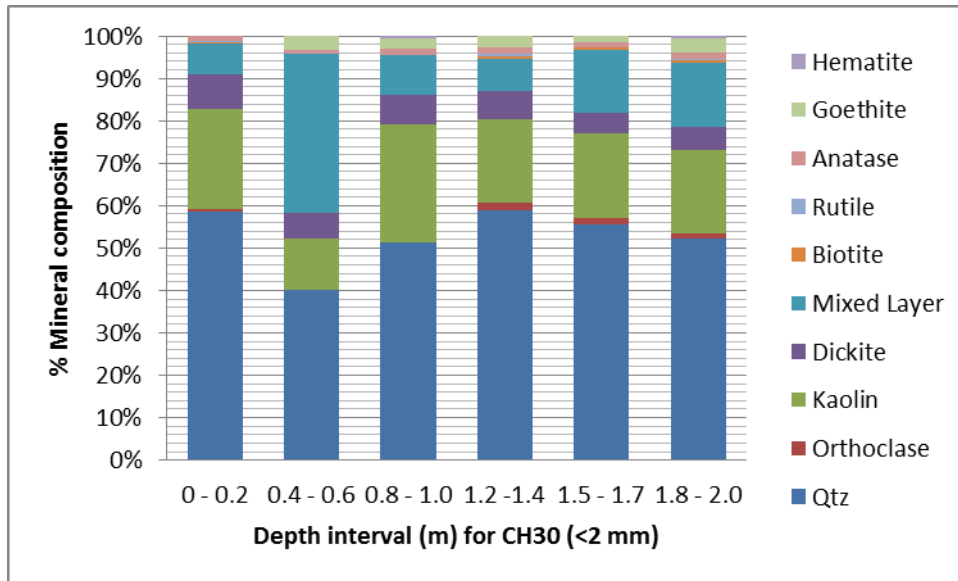


Figure 4.9: Mineralogical composition of the < 2 mm fraction of CH30 corehole samples at various depth intervals determined by XRD analysis.

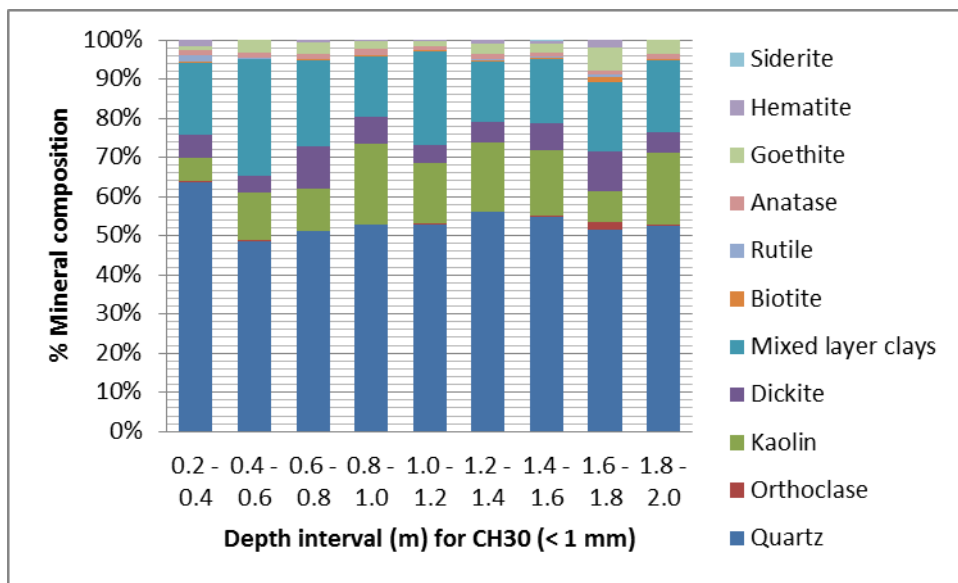


Figure 4.10: Mineralogical composition of the < 1 mm fraction of CH30 corehole samples at various depth intervals determined by XRD analysis.

With the exception of the W2D topsoil, the mineralogical assessment of the W2D samples were performed on subsamples of the bulk material (i.e. subsamples were not sieved to recover only the < 2 mm fraction). The W2D samples have ca. 30% quartz in the first meter of core below the ground surface. Below two meters from the ground surface, the quartz content ranges from 50 – 70% with depth. The oxide content is significant in the top meter ranging from 18 – 35%. Siderite is also prevalent at depths below 6 m, ranging from 5 to 18%. The presence of siderite is supported by the higher natural pH observed for soils at the 6.5 and 9.5 m depth interval (Section 4.2.1).

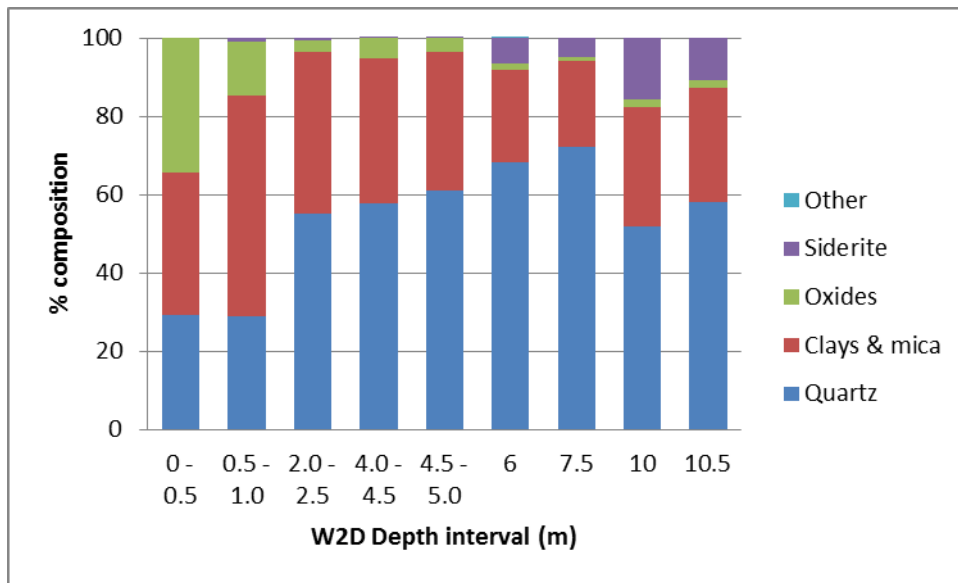


Figure 4.11: Percentage composition of quartz, clays & mica and oxides in W2D samples for various depth intervals.

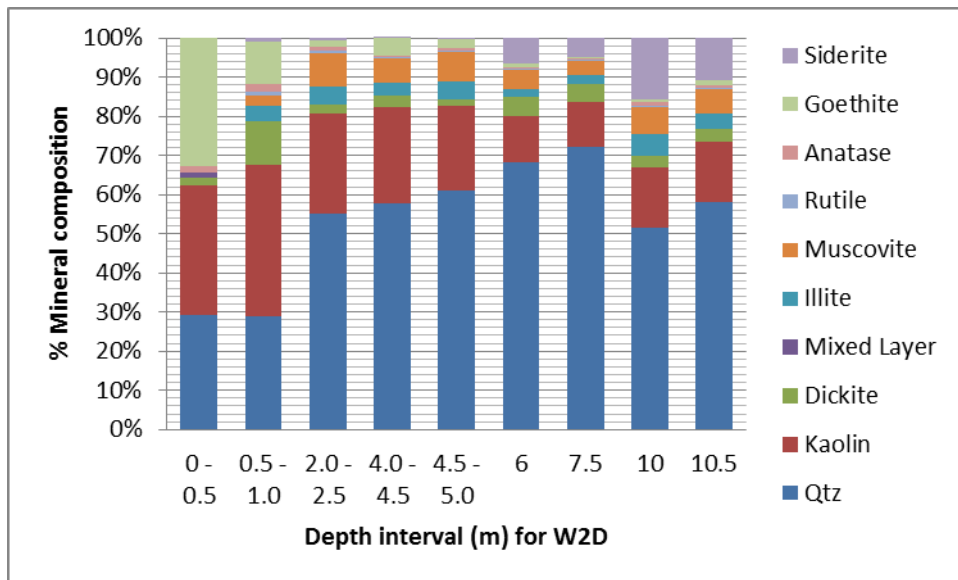


Figure 4.12: Mineralogical composition of the W2D samples at various depth intervals as determined by XRD analysis.

The present data shows that the mineralogy across the site is heterogeneous. While it is noted that CH1A has lower amounts of quartz compared to the other locations, the mineralogical data for CH1A presents a better estimate of the phase identification of the clays as orientation of the samples and pretreatment were used to purposefully identify the clays. The higher values for quartz for the other LFLS samples are more typical of estimates in the Sydney Basin for shale lenses within the Hawkesbury sandstone (per comm – Cendon, June 2016).

Early records describe the soils of the site as highly weathered and derived from the shale layer which is generally weathered to a depth of 6 m, resulting in a profile from surficial red-brown clay soil, through mottled grey and silty kaolinite clay with numerous fine sandy partings. Immediately below the soil and weathered material lies light grey leached silty shale grading to fresh dark carbonaceous parent shale with silty interbedding [Isaac and Mears, 1977]. Early records also report the clay in the Lucas Heights area is likely to average 40% SiO₂, 30% kaolinite, and 30% illite [Bradd, 2003]. An assessment of the content of these major mineral groups for the clays in the present study is summarized in Table 4.4. The data in Table 4.4 clearly shows the heterogeneity between clay samples both vertically and laterally at the LFLS site.

Table 4.4: Major mineral groups in LFLS clays from CH1A, CH30 and W2D cores

COREHOLE	Depth (m)	Number of samples	SiO ₂ (%)	Kaolin/dickite (%)	Illite/ smectite/mica /muscovite (%)
CH1A	0.4 - 1.6	2	25 - 28	28-31	37 - 46
CH30	0.2 - 1.6	10	40 - 64	12 - 34.6	7.6 - 37.5
W2D	0.5 - 5	4	29 - 61	23.5 - 50	6.4 - 13

5. Sorption studies of Co, Cs and Sr onto soils

5.1. Radiotracers

The radiotracers Cs-137, Co-57 and Sr-85 were purchased from Eckert & Ziegler as carrier-free solutions. Isotopic stock solutions were diluted with 0.1 M HCl to prepare 10 kBq mL⁻¹ working solutions.

5.2. Batch sorption method

The batch sorption studies were performed in Nalgene centrifuge tubes with a 2 mm hole in the lid to allow air equilibration. These experiments were conducted on selected materials with a mass loading of 10 g/L, an initial activity of ca. 500 Bq of each radiotracer and ionic strength of 0.01 M (NaCl). All experiments were conducted at 25 °C. To investigate the effect of ionic strength on sorption, sorption studies were also conducted on four samples from CH1A at an ionic strength of 0.1 M NaCl. NaCl was chosen as the matrix as most of the groundwater in the vicinity of the trenches at LFLS is of the Na-Cl type [Cendon et al., 2015].

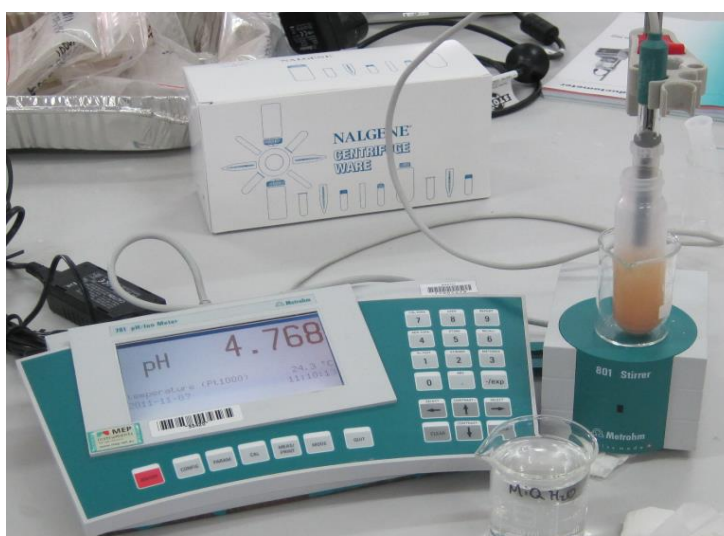


Fig. 5.1: Set-up for pH determination of a sorption sample

The solid and aqueous phases were equilibrated for a minimum of 16 h in a temperature controlled shaking water bath at the desired equilibrium pH (target pH) prior to the addition of tracer. In some cases, the equilibration time was extended for much longer periods (several days) to ensure a stable target pH prior to addition of radionuclide tracer. For some samples, the solid and aqueous phases were initially pre-equilibrated without any pH adjustment for several days prior to adjustment to the target pH and subsequent equilibration. After the pre-equilibration at the target pH, the radionuclide tracer was subsequently added and the pH adjusted back to the target pH. The experimental equilibration time was 48 h however, the pH was checked after 24 h and pH adjusted to the target pH, if required, by addition of dilute NaOH or HCl. A combined pH electrode (Metrohm) was used for pH measurements (Fig. 5.1). At completion of the radionuclide equilibration, the final pH was determined for each sorption sample. The aqueous phase was separated by high speed centrifugation at 8000 g for 20 minutes and a 10 mL aliquot subsampled and subsequently acidified to pH < 2 prior to analysis.

5.3. Analysis of sorption samples

5.3.1. Gamma analysis

The Co, Sr and Cs activities were measured by gamma spectrometry using an ORTEC High-Purity Germanium (HPGe) n-type reduced background detector coupled to an ORTEC DSPEC Pro with MAESTRO software.

5.3.2. ICP analysis

Following gamma counting, the aqueous sub-samples were analysed for major metals and minor elements of interest by Inductively Coupled Plasma - Atomic Emission Spectrometry (ICP-AES) and Inductively Coupled Plasma - Mass Spectrometry (ICP-MS).

5.4. Sorption results for Co, Cs and Sr

5.4.1. Sorption of Co, Cs and Sr for all LFLS samples

The sorption curves for Co, Cs and Sr as a function of pH and at an ionic strength of 0.01 M (NaCl) are shown in Figure 5.2 for over 70 samples of LFLS soils. A compilation of sorption data can be found in Appendix 2. The sorption of Cs typically ranges from 80 to 100 % for LFLS materials and is pH independent whereas the sorption of Co and Sr are pH dependent with a sorption edge between pH 4 and 6. At pH > 6, the sorption of Co nears maximum (i.e. 100%) for the majority of samples, while the sorption of Sr typically ranges from 50 to 90%.

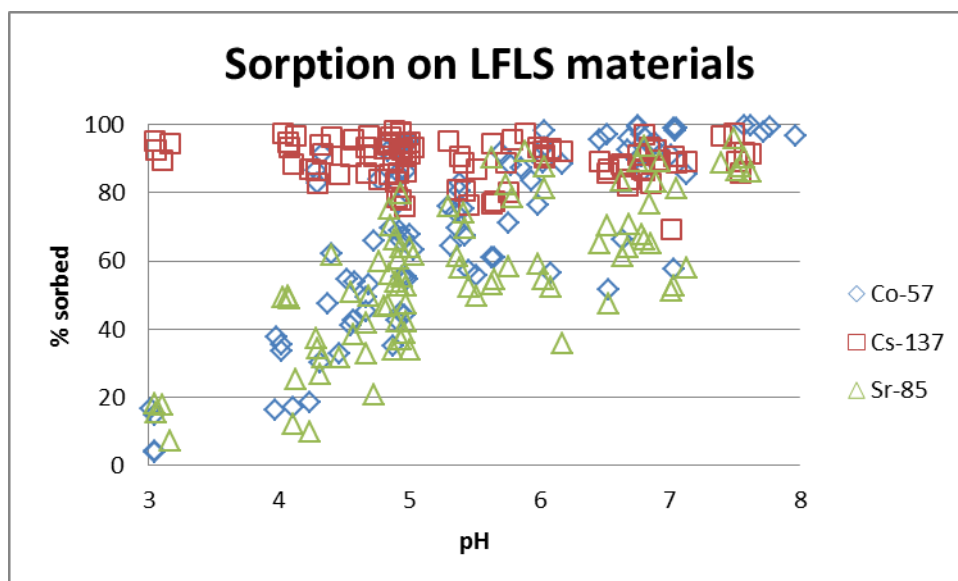


Figure 5.2: Sorption curves for sorption of Co, Cs and Sr onto topsoil and unconsolidated LFLS materials (soils) as a function of pH. Mass loading of 10 g/L; Ionic strength 0.01 M; air equilibration; T = 25°C.

5.4.2. Sorption curves as a function of lithologies

Figure 5.3 to 5.9 show the sorption curves obtained for Co, Sr and Cs for the various lithological units of LFLS soils. The pH dependence for Co and Sr is most apparent for the LFLS clays (i.e. silty clays, clays and shaley clays) and the shale material.

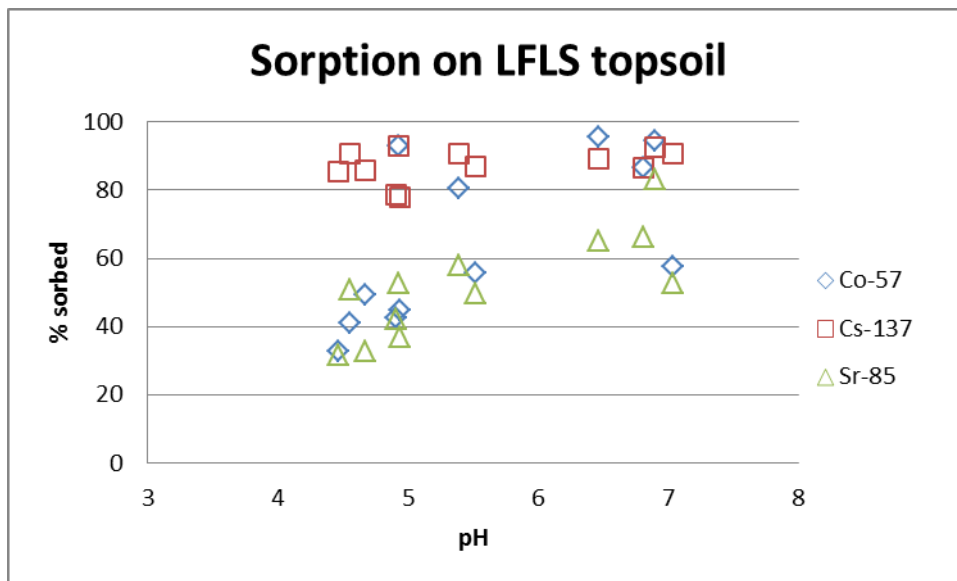


Figure 5.3: Sorption curves for sorption of Co, Cs and Sr onto LFLS topsoils CH1 (0 – 0.20 m), CH30 (0 – 0.20 m) and W2D (0 – 0.5 m) as a function of pH. Mass loading of 10 g/L; ionic strength 0.01 M; air equilibration; T = 25°C.

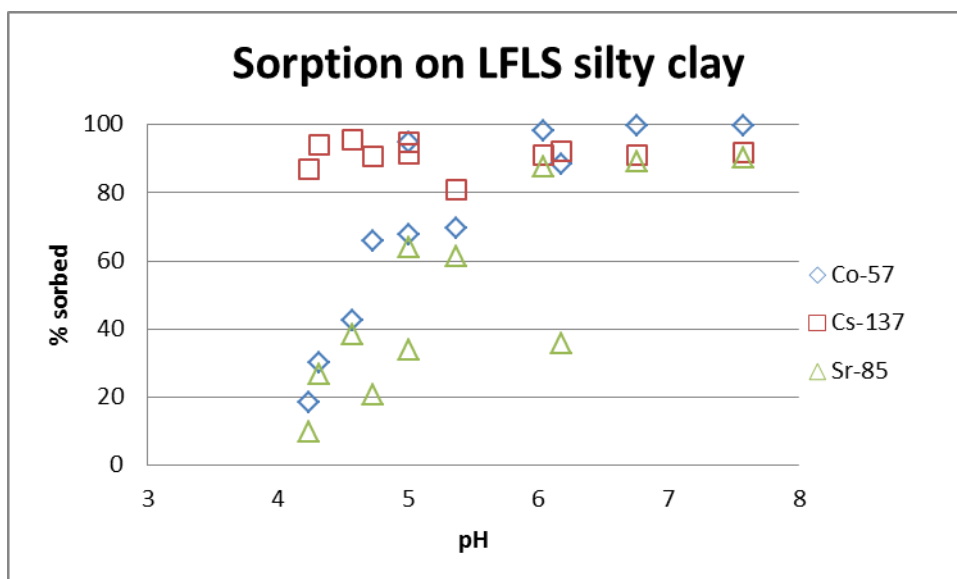


Figure 5.4: Sorption curves for sorption of Co, Cs and Sr onto LFLS silty clays CH30 (0.2 – 0.4 m); W2D (1.0 – 1.5 m) as a function of pH. Mass loading of 10 g/L; ionic strength 0.01 M; air equilibration; T = 25°C.

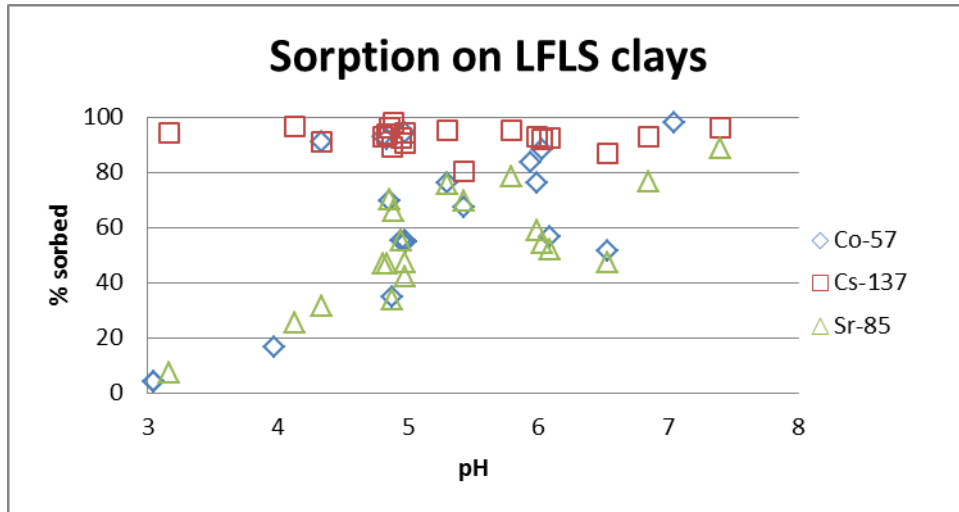


Figure 5.5: Sorption curves for sorption of Co, Cs and Sr onto LFLS clays CH1A (0.4 – 0.6 m); CH30 (0.4 – 1.0 m), W2D (4.5 – 5.0 m) as a function of pH. Mass loading of 10 g/L; Ionic strength 0.01 M; air equilibration; T = 25°C.

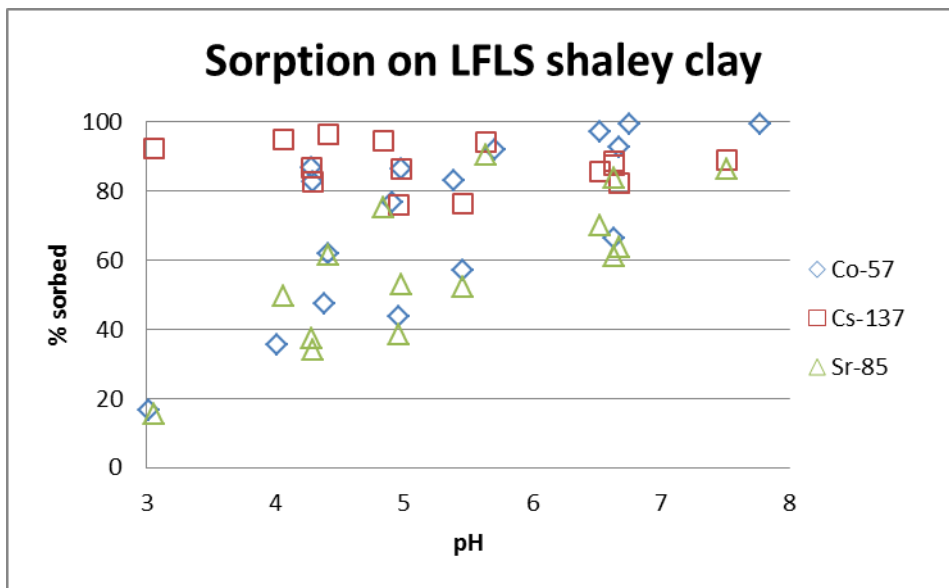


Figure 5.6: Sorption curves for sorption of Co, Cs and Sr onto LFLS shaley clays CH1A (1.4 – 1.6 m), CH30 (1.0 – 1.2 m) as a function of pH. Mass loading of 10 g/L; Ionic strength 0.01 M; air equilibration; T = 25°C.

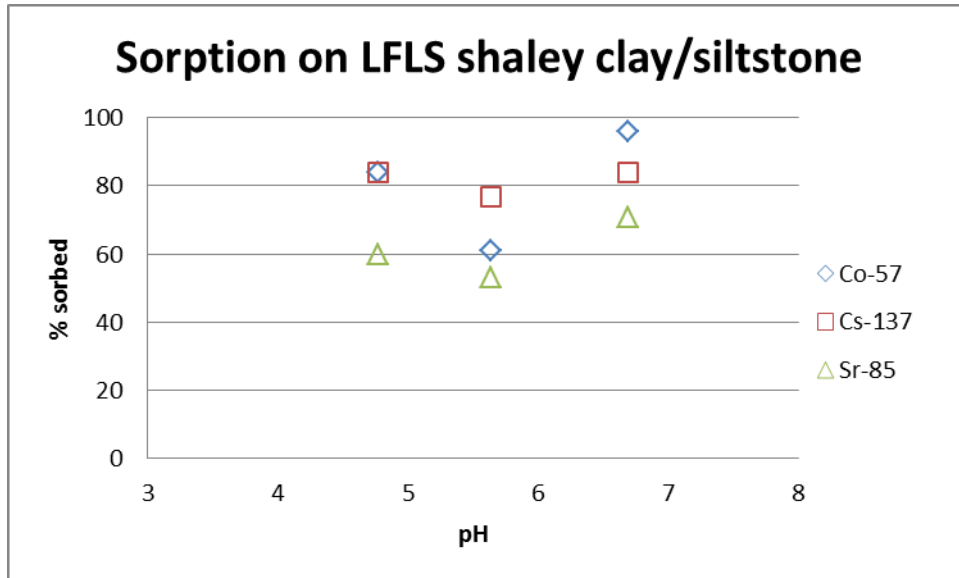


Figure 5.7: Sorption curves for sorption of Co, Cs and Sr onto LFLS shaley clay/siltstone CH30 (1.4 – 1.6 m) as a function of pH. Mass loading of 10 g/L; ionic strength 0.01 M; air equilibration; T = 25°C.

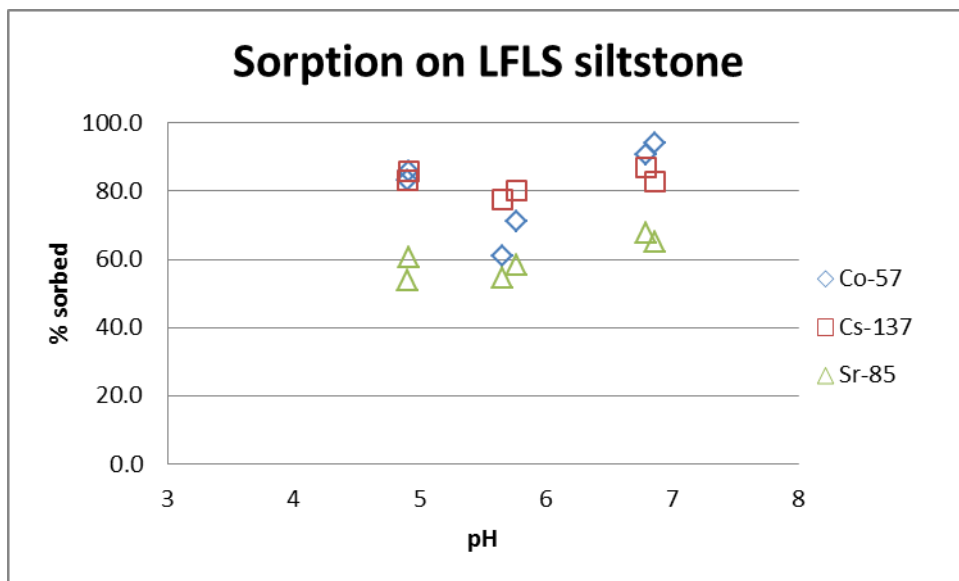


Figure 5.8: Sorption curves for sorption of Co, Cs and Sr onto LFLS siltstone (1.6 – 1.8 m); as a function of pH. Mass loading of 10 g/L; ionic strength 0.01 M; air equilibration; T = 25°C.

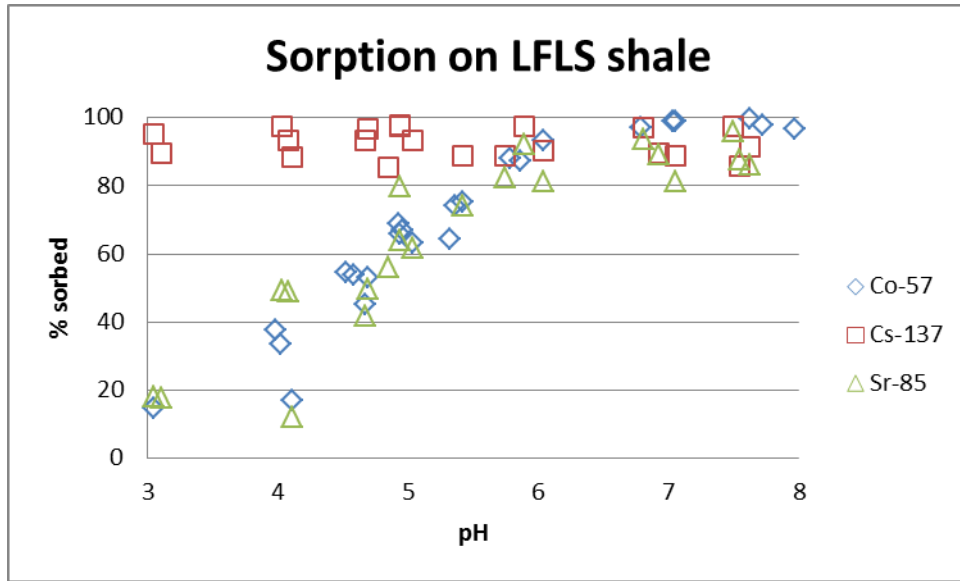


Figure 5.9: Sorption curves for sorption of Co, Cs and Sr onto LFLS shale CH1A (2.4 – 2.6 m; 3.4 – 3.0 m); W2D (2.5 – 3.0 m) as a function of pH. Mass loading of 10 g/L; Ionic strength 0.01 M; air equilibration; T = 25°C.

5.4.3. Effect of ionic strength on sorption by CH1A samples.

The effect of ionic strength on sorption was investigated using four samples of CH1A at the various depth intervals and at two ionic strengths, namely 0.01 M and 0.1 M (NaCl). Figure 5.10 shows the sorption curves obtained for Cs, Sr and Co, respectively, as a function of pH for the two ionic strengths. The sorption of Cs ranges from 82% to 98%, with no strong pH or ionic strength dependence.

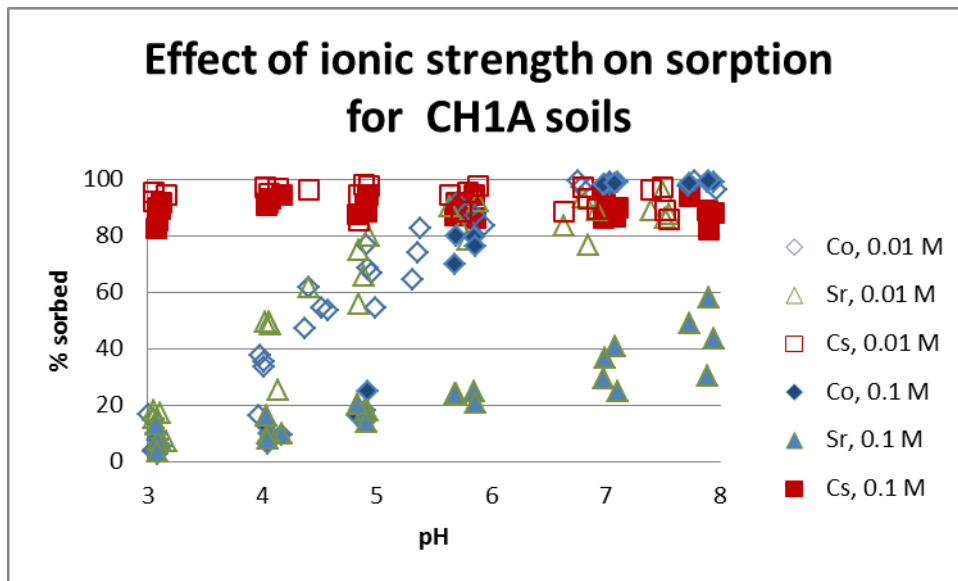


Fig. 5.10: Sorption of Co, Sr and Co onto CH1A soils (mass loading = 10 g/L; equilibrium with air; 25 °C) at two ionic strengths. Filled symbols are at the low ionic strength and open symbols are at the high ionic strength.

However, there is a strong pH and ionic strength dependence for Sr whereby the sorption of Sr is significantly reduced over the entire pH range at the higher ionic strength, with a maximum sorption of < 60%. At pH > 6, maximum sorption (ca. 100%) is obtained at both ionic strengths.

The sorption of Sr at the lower ionic strength shows a greater pH dependency relative to the sorption at higher ionic strength in the pH range 3 to 6. Above pH 6, maximum sorption of ca. 90 to 95% is attained. An ionic strength dependency is also observed for pH values > 4, whereby Sr sorption is significantly reduced at the higher ionic strength. The sorption curves at the higher ionic strength are much shallower in the pH range 3 to 8 with a maximum sorption of < 60% at pH 8.

The sorption of Co is pH dependent at both ionic strengths. At the lower ionic strength, the soil samples have a pH_{50} (i.e. pH of 50% adsorption) of around 4.5. For pH values below 6, the sorption curves are similar for all samples at the higher ionic strength and sorption is typically lower than at the corresponding pH value for the lower ionic strength. The pH_{50} is shifted by ca. one pH unit to the right. All materials reach maximum sorption (ca. 100%) above pH 6.5.

6. Estimates of Distribution Coefficients (K_d) for Co, Cs and Sr at LFLS

The distribution coefficient (K_d value) is the ratio of the radionuclide concentration adsorbed by the solid (C_s) and the concentration in the liquid (C_l), given by

$$K_d = C_s / C_l \quad (1)$$

The K_d approach takes no explicit account of sorption mechanisms but assumes that the radionuclide on the solid phase is in equilibrium with the radionuclide in solution and that exchange between these phases is reversible [IAEA 2010].

6.1. Estimates of K_d from LFLS sorption data

The K_d values have been estimated from the sorption data in the present work. Compilations of K_d data for the subsamples are provided in Appendix 2.

For the ensuing plots of K_d values vs pH (Figs. 6.1 – 6.8), and the summary tables (Tables 6.1 – 6.3), some assumptions have been made as follows:

- the K_d s are deduced from sorption data, typically in the pH range between 4 and 8 so as to be relevant to site conditions [Cendon, 2015].
- Where sorption was > 97.5%, the K_d values are not included in the plots nor for estimates of the mean and standard deviation values (arithmetic and geometric) reported in Tables 6.2 and 6.3. As the amount sorbed relies on a measurement of the equilibrium solution concentration (C_l), there is greater uncertainty in this measurement when sorption approaches the maximum value of 100% as the value of C_l would be very low. Hence a conservative uncertainty estimate of 2.5% has been adopted setting an upper bound for absorption at 97.5%, and therefore an upper limit K_d value of ca. 4000 L/kg. Note however, that all K_d estimates are included in the compilation data in Appendix 2.
- A separate Table has been provided for K_d estimates for topsoil/fill due to the topdressing activities that have been undertaken to address subsidence at the site [Payne, 2012]. These may have involved soil materials from beyond the immediate vicinity of LFLS.
- The Tables in the following section provide both the arithmetic mean and geometric mean, and their respective standard deviations. It is recommended that the geometric mean values are used for dose modelling since K_d values in each category (lithologies) will be dependent on a range of factors (e.g. pH, grain size, mineralogy, etc.) and therefore better represented by a geometric mean value.

6.1.1. Kd values for Co, Sr and Cs for LFLS materials

Kd values have been estimated for all LFLS soils (Figure 6.1) and for the different lithologies (Figures 6.2 – 6.8).

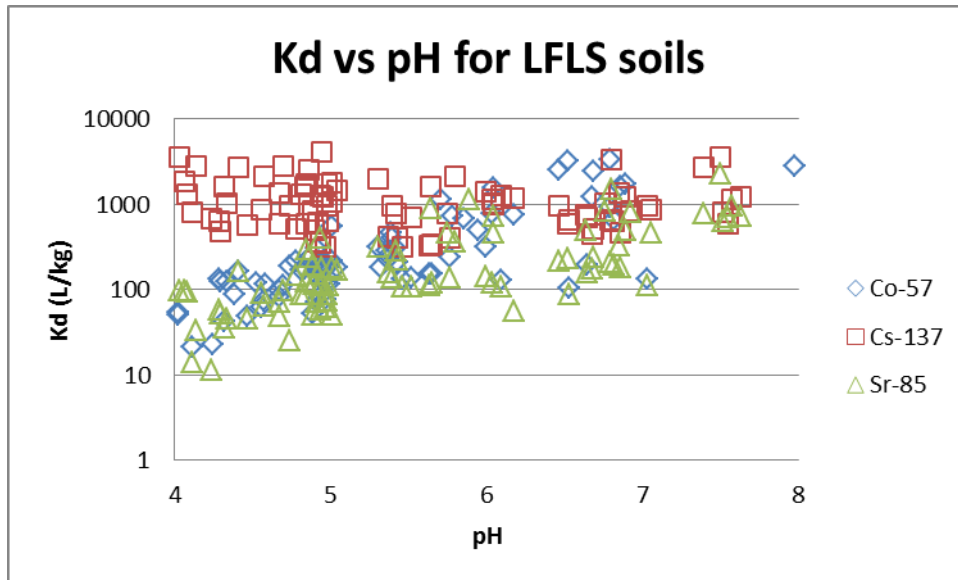


Figure 6.1: Kd values for Co, Sr and Cs vs pH for topsoil and unconsolidated LFLS materials (CH1 (0 – 20 cm), CH1A (0.4 – 0.6 m, 1.4 – 1.6 m, 2.4 – 2.6 m, 3.4 – 3.6 m), CH30 (0 – 2 m); W2D (0 – 50 cm, 1 – 1.5 m, 2.5 – 3.0 m, 4.5 – 5.0 m). Mass loading of 10 g/L; ionic strength 0.01 M; air equilibration; T = 25°C.

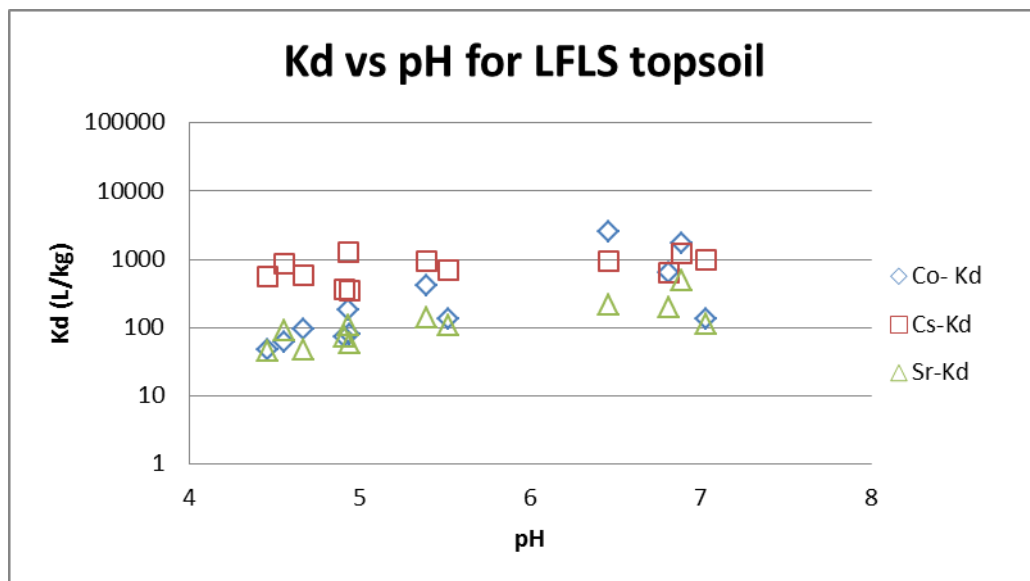


Figure 6.2: Kd for Co, Sr and Cs vs pH for LFLS topsoils CH1 (0 – 0.20 m), CH30 (0 – 0.20 m) and W2D (0 – 0.5 m). Mass loading of 10 g/L; ionic strength 0.01 M; air equilibration; T = 25°C.

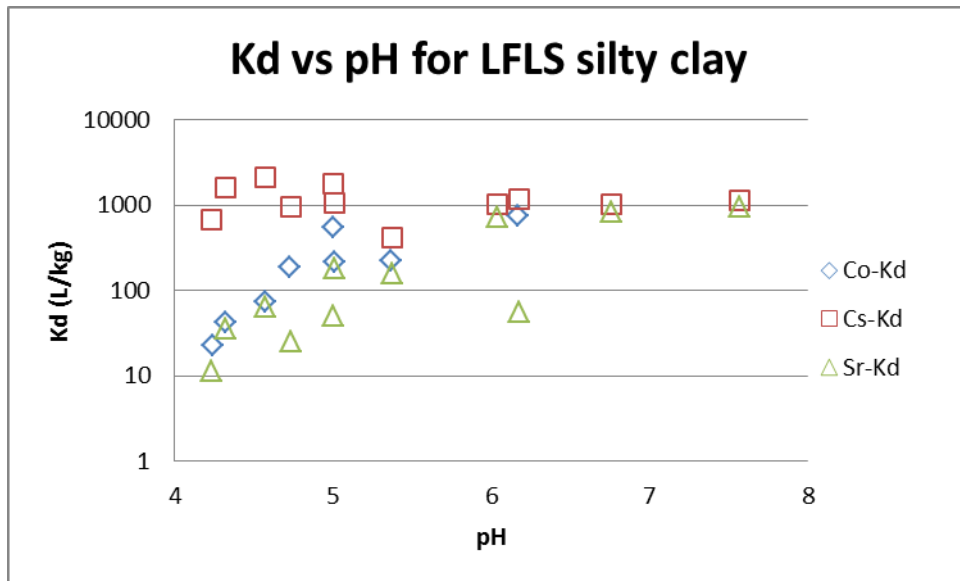


Figure 6.3: Kd for Co, Sr and Cs vs pH for LFLS silty clays CH30 (0.2 – 0.4 m); W2D (1.0 – 1.5 m). Mass loading of 10 g/L; ionic strength 0.01 M; air equilibration; T = 25°C.

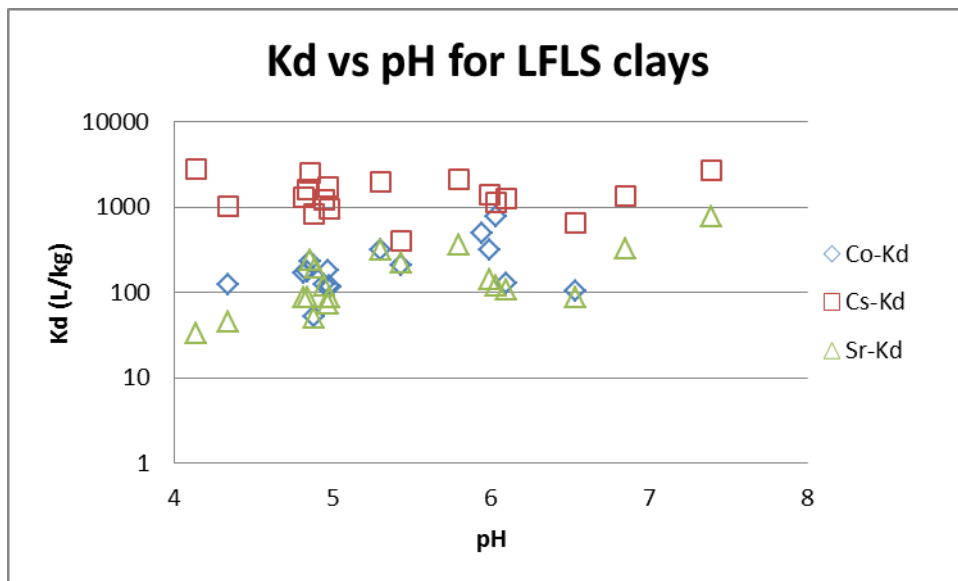


Figure 6.4: Kd for Co, Sr and Cs vs pH for LFLS clays CH1A (0.4 – 0.6 m); CH30 (0.4 – 1.0 m), W2D (4.5 – 5.0 m). Mass loading of 10 g/L; ionic strength 0.01 M; air equilibration; T = 25°C.

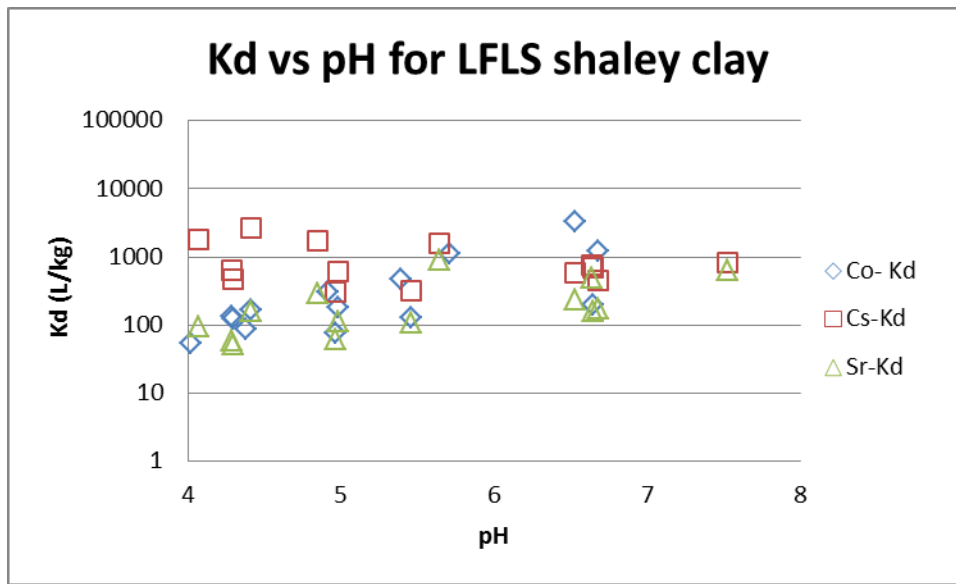


Figure 6.5: Kd for Co, Sr and Cs vs pH for LFLS shaley clays CH1A (1.4 – 1.6 m), CH30 (1.0 – 1.2 m). Mass loading of 10 g/L; Ionic strength 0.01 M; air equilibration; T = 25°C.

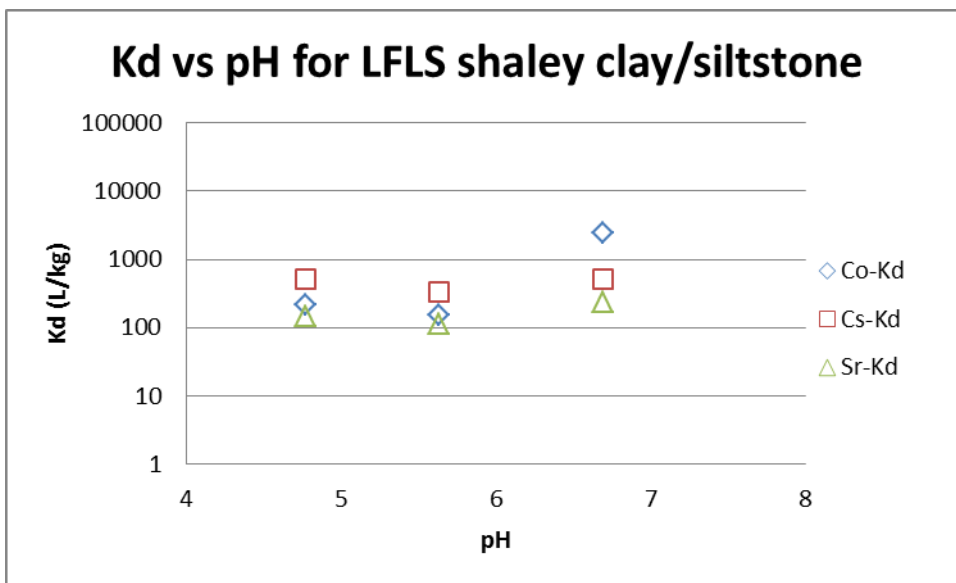


Figure 6.6: Kd for Co, Sr and Cs vs pH for LFLS shaley clay/siltstone CH30 (1.4 – 1.6 m). Mass loading of 10 g/L; Ionic strength 0.01 M; air equilibration; T = 25°C.

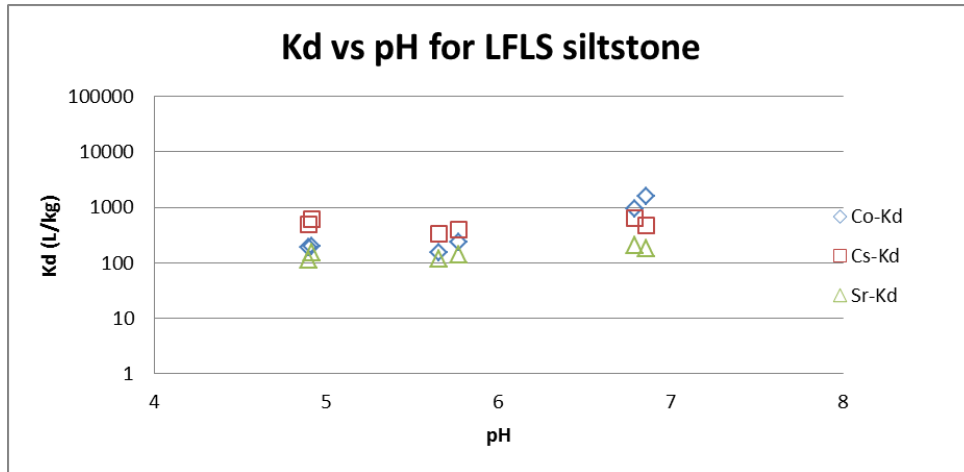


Figure 6.7: Kd for Co, Cs and Sr vs pH for LFLS siltstone (1.6 – 1.8 m); Mass loading of 10 g/L; Ionic strength 0.01 M; air equilibration; T = 25°C.

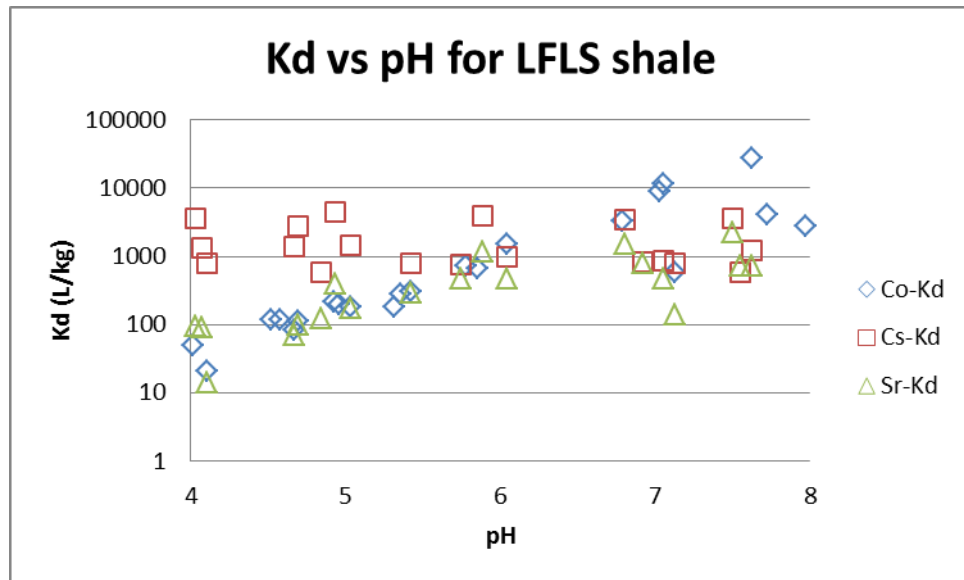


Figure 6.8: Kd for Co, Cs and Sr vs pH for LFLS shale CH1A (2.4 – 2.6 m; 3.4 – 3.0 m); W2D (2.5 – 3.0 m). Mass loading of 10 g/L; Ionic strength 0.01 M; air equilibration; T = 25°C.

Tables 6.1 – 6.3 presents a summary of the average K_d values (AM = arithmetic mean and GM =geometric mean) and their respective standard deviations, for all soils and for the various lithological units, as well as the range of K_d values determined (Low = lowest K_d , High =highest K_d), and the number of data points used for the determination (N). The topsoil data has been presented in a separate Table due to the possibility that soils from an external site other than LFLS may have been used in topdressing in the vicinity of the legacy trenches.

The average K_d value for Cs sorption for LFLS topsoil/fill (N = 12) is 730 L/kg with a GSD of 1.5. The average K_d for Co is 210 L/kg (GSD = 3.7) and the average K_d for Sr is 120 L/kg (GSD = 2.0).

Table 6.1: K_d values for Co, Sr and Cs for LFLS Topsoil/Fill

LITHOLOGY	COREHOLE	DEPTH (m)		Kd (L/kg)		
				Co	Sr	Cs
TOPSOIL/FILL			AM	510	140	780
	CH1	0 - 0.2	Std dev	790	120	300
	CH30	0 - 0.2	LOW	48	45	350
	W2D	0 - 0.5	HIGH	2500	500	1300
			GM	210	110	730
			GSD	3.7	2.0	1.5
			N	12	12	12

KEY:

AM – arithmetic mean

Std dev – standard deviation of the mean

LOW – lowest K_d value in sample set

HIGH – highest K_d value in sample set

GM – geometric mean

GSD – standard deviation of geometric mean

N – number in sample set

K_d s were estimated from batch sorption studies. Ionic strength = 0.01 M, Mass loading of 10 g/L.

K_d values estimated for pH range 4 – 8 for Co, Cs and Sr with average pH of 5.5 (GSD = 1.2).

Excluding the topsoil/fill data, the average K_d value for Cs sorption for all other LFLS soils (N = 66) was 1000 L/kg with a GSD of 1.9. The shaley clay and/or siltstone samples had the lowest average K_d values (440 – 770 L/kg) whereas the average K_d values for Cs for the clay and shale materials were the highest and similar (1300 L/kg, 1400 L/kg, respectively). The average K_d values for Co and Sr (N = 65) were significantly lower than that for Cs for all LFLS soils and similar at 210 L/kg and 180 L/kg. The highest K_d s for Co was observed for the shaley clay/siltstone and siltstone materials at 430 L/kg and 360 L/kg, respectively. The highest K_d for Sr was observed for the shale material at 290 L/kg, whereas the K_d for the clay and siltstone materials ranged from 130 – 170 L/kg.

Table 6.2: Kd values for Co, Sr and Cs for LFLS lithological units

LITHOLOGY	COREHOLE	DEPTH (m)		Kd (L/kg)		
				Co	Sr	Cs
SILTY CLAY	W2D	1 - 1.5	AM	120	370	1100
			Std dev	97	390	530
			LOW	23	11	410
			HIGH	230	950	2100
			GM	81	160	1000
			GSD	2.7	5.0	1.6
			N	5	8	8
CLAY	CH1A	0.4 - 0.6	AM	210	180	1500
			Std dev	180	170	680
	CH30	0.4 - 1.0	LOW	18	33	410
			HIGH	770	780	2800
	W2D	4.5 - 5.0	GM	160	130	1300
			GSD	2.3	2.2	1.6
			N	17	19	18
SHALEY CLAY	CH1A	1.4 - 1.6	AM	540	250	960
			Std dev	870	250	700
	CH30	1.0 - 1.4	LOW	53	52	310
			HIGH	3300	890	2700
			GM	240	170	770
			GSD	3.3	2.4	2.0
			N	14	14	14
SHALEY CLAY/SILTSTONE	CH30	1.4 - 1.6	AM	940	170	450
			Std dev	1300	66	110
			LOW	150	110	330
			HIGH	2400	240	520
			GM	430	160	440
			GSD	4.5	1.5	1.3
			N	3	3	3
SILTSTONE	CH30	1.6 - 2.0	AM	550	150	490
			Std dev	590	36	120
			LOW	150	110	230
			HIGH	1600	210	650
			GM	360	150	480
			GSD	2.7	1.3	1.3
			N	6	6	6
SHALE			AM	590	530	1700
			Std dev	930	580	1200
			LOW	21	14	580
	CH1A	2.4 - 2.6; 3.4 - 3.6	HIGH	3300	2300	4100
			GM	240	290	1400
	W2D	2.5 - 3	GSD	3.8	3.5	2.0
			N	19	19	17
ALL SOILS	CH1A	see above	AM	450	310	1300
			Std dev	730	380	890
			LOW	18	11	310
			HIGH	3300	2300	4100
			GM	210	180	1000
			GSD	3.2	2.9	1.9
			N	64	69	66

KEY:

AM – arithmetic mean

Std dev – standard deviation of the mean

LOW – lowest Kd value in sample set

HIGH – highest Kd value in sample set

GM – geometric mean

GSD – standard deviation of geometric mean

N – number in sample set

Kds were estimated from batch sorption studies. Ionic strength = 0.01 M, Mass loading of 10 g/L.

Kd values estimated for pH range 4 – 8 for Co, Cs and Sr with average pH of 5.4 (GSD = 1.2).

Kd values for samples with > 97.5% sorption have not been included in this table. Refer to Appendix for these values.

6.1.2. Effect of Ionic strength on Kd values for Co, Sr and Cs for CH1A soils

A comparison of average Kd values for Co, Sr and Cs at two ionic strengths (0.01M and 0.1 M) for CH1A soils is given in Table 6.3. The soils have been classed according to lithology and average Kd values estimated for each lithology as well as average values for all shale, and for all soils combined. For Co, Sr and Cs, the Kd is highest at the lower ionic strength, which suggests that these radionuclides are more mobile at the higher ionic strength. The pH values of the soils range from pH 4 to pH 8 with an average GM of 5.4 (GSD=1.2) at 0.01 M and an average GM of 5.2 (GSD = 1.5) at 0.1 M.

The samples at interval 2.4 – 2.6 m and 3.4 – 3.6 m are both classified as shales yet have very different sorption properties for Cs at the lower ionic strength. The Kd for Cs for the upper layer of shale is significantly lower (780 L/kg) compared to the Kd for Cs for the bottom layer (3500 L/kg). However, this disparity is not observed at the higher ionic strength (730 vs 690 L/kg). The Kd for Sr at the lower ionic strength for the uppermost shale layer is also significantly different to that for the lower layer shale (310 vs 680 L/kg). A possible explanation for this is that the uppermost shale layer has a lower fine clay fraction compared to the other samples as seen in Figure 4.2. The lower shale layer has the highest mica and/or illite component (ca. 11% vs 6 to 8%) which may explain the higher Cs sorption for this layer. The lower layer shale also has a slightly higher iron oxide content compared to the upper layer shale, hence providing more sorption sites.

The average Kd value for Cs at the lower ionic strength is 1500 L/kg and 960 L/kg at the higher ionic strength. The average Kd values for Co and Sr increase with depth at the lower ionic strength, ranging from 100 to 300 L/kg (GM of 230 L/kg) and 230 to 680 L/kg (GM of 350 L/kg), respectively. There is no significant increase observed with depth at the higher ionic strength. The average Kd values for Co and Sr at the higher ionic strength are 42 L/kg and 31 L/kg, respectively.

Table 6.3: Kd values for Co, Sr and Cs for CH1A lithological units at low and high ionic strengths

CH1A			Kd (L/kg)					
LITHOLOGY	DEPTH (m)		Co		Sr		Cs	
			0.01 M	0.1 M	0.01 M	0.1 M	0.01 M	0.1 M
CLAY	0.4 - 0.6	AM	210	140	340	43	2200	1600
		Std dev	250	210	280	33	650	100
		LOW	18	6	33	11	1300	1500
		HIGH	490	380	780	94	2800	1700
		GM	100	51	230	33	2100	1600
		GSD	5.2	6.3	3.3	2.3	1.4	1.1
		N	3	3	5	5	4	5
SHALEY CLAY	1.4 - 1.6	AM	370	140	430	28	1600	1000
		Std dev	400	220	300	12	710	210
		LOW	53	11	97	12	760	800
		HIGH	1100	390	890	43	2700	1300
		GM	220	46	330	26	1400	1000
		GSD	3.1	6.7	2.3	1.6	1.6	1.2
		N	6	3	6	5	6	5
SHALE	2.4 - 2.6	AM	760	87	440	35	820	740
		Std dev	1300	120	320	23	300	140
		LOW	50	14	92	15	580	660
		HIGH	3300	230	790	78	1300	980
		GM	280	40	310	35	780	730
		GSD	4.4	4.6	2.7	1.7	1.4	1.2
		N	6	3	5	5	5	5
SHALE	3.4 - 3.6	AM	680	110	1100	51	3500	720
		Std dev	1000	180	870	53	130	250
		LOW	60	7	96	9	3400	450
		HIGH	2800	320	2300	140	3600	1100
		GM	300	33	680	32	3500	690
		GSD	3.9	7.4	3.6	3.0	1.0	1.4
		N	6	3	5	5	3	5
ALL SHALE	2.4 - 2.6 and 3.4 - 3.6	AM	720	100	760	45	1800	730
		Std dev	1100	140	700	39	1400	190
		LOW	50	7	92	9	580	450
		HIGH	3300	390	2300	140	3600	1100
		GM	290	37	460	33	1400	710
		GSD	3.9	4.9	3.2	2.3	2.3	1.3
ALL SOILS	see above	N	12	6	10	10	8	10
		AM	550	120	560	40	1800	1000
		Std dev	870	160	550	32	1100	420
		LOW	50	7	92	9	580	450
		HIGH	2800	390	2300	140	3600	1700
		GM	230	42	350	31	1500	960
		GSD	3.7	4.8	2.9	2.1	1.9	1.5
		N	21	12	21	20	18	20

KEY:

AM – arithmetic mean

Std dev – standard deviation of the mean

LOW – lowest Kd value in sample set

HIGH – highest Kd value in sample set

GM – geometric mean

GSD – standard deviation of geometric mean

N – number in sample set

Kds were estimated from batch sorption studies. Mass loading of 10 g/L.

Kd values estimated for pH range 4 – 8 for Co, Cs and Sr with average pH of 5.4 (GSD = 1.2) at 0.01 M NaCl and average pH of 5.2 (GSD = 1.5) at 0.1 M NaCl, respectively.

Kd values for samples with > 97.5% sorption have not been included in this table. Refer to Appendix for these values.

6.2. Comparison of Kd values with historical site data

There has been only one set of previously reported Kd values for Co, Cs and Sr at the LFLS by Isaac and Mears [1977] in their report titled 'A study of the burial ground used for radioactive waste at the Little Forest Area near Lucas Heights New South Wales'. This report describes laboratory and field work connected with the study of the fate of radionuclides buried at the site [AAEC/E427, 1977]. A description of the samples and some of their work on the cation exchange capacity (CEC) of these materials were described in Section 4.2.2 and Table 4.2 of the present study. The Kd values were determined by batch experiments using borehole waters of different ionic concentrations and pH. A soil/liquid ratio of 0.05 g/L was used and the distribution coefficients were determined on 1 g soil samples (0.25 – 0.5 mm size) after equilibration with three 10 mL portions of filtered borehole water. The soil samples were washed with alcohol, dried at 80 °C and subsequently contacted with 20 mL of filtered borehole water containing the tracer of interest. While Isaac and Mears utilised Co-60 and the present work has utilised Co-57 for the sorption studies, the chemical behaviour of both isotopes will be the same. The borehole water was sourced from two boreholes, representing bore water at low ionic strength (borehole BH10) and bore water at high ionic strength (borehole BHB). The former has a chloride concentration of 1200 mg/L (~0.03 M) and a pH of 7.0 and the latter has a chloride concentration of 3370 mg/L (~0.1 M) and pH of 5.0. The latter is therefore comparable to our experimental conditions with high ionic strength of 0.1 M and average pH of 5.2.

The distribution coefficients of the cations Co-60, Cs-137 and Sr-85 using borehole water is summarised in Table 6.4.

Table 6.4: Summary of Distribution Coefficients of cations Co-60, Cs-137 and Sr-85 using borehole water in Isaac and Mears study (1977).

Soil Fraction	Kd (L/kg)					
	Co-60		Cs-137		Sr-85	
	Low IS pH 7.0	High IS pH 5.0	Low IS pH 7.0	High IS pH 5.0	Low IS pH 7.0	High IS pH 5.0
F1	38	9	3700	2900	11	1
F2	7	3	2100	2100	9	1
F3	5	2	2500	3600	7	1
F4	5	2	1600	2700	7	1

Low IS: BH10 borehole water, pH 7.0. Initial concentrations: Ca²⁺:13 mg/L; Na⁺:840 mg/L; K⁺: 11 mg/L; Al³⁺: < 0.1 mg/L; Mg²⁺: 73 mg/L; Cl⁻: 1200 mg/L

High IS: BHB borehole water, pH 5.0. Initial concentrations: Ca²⁺:170 mg/L; Na⁺:2000 mg/L; K⁺: 24 mg/L; Al³⁺: 0.7 mg/L; Mg²⁺: 320 mg/L; Cl⁻: 3370 mg/L

It is noted that the soil samples used in the study by Isaac and Mears have significantly more kaolinite than any of the samples used in our present study. This may be due to the selective fractionation of the samples by Isaac and Mears whereby their particle size range (0.25 – 0.5 mm) excludes the clay and silt fraction. The methodology and experimental conditions used by Isaac and Mears is also significantly different to that used in our present study so results cannot be directly compared. However, both studies are consistent in showing that the Kd values for Cs are significantly higher than that for Co and Sr.

6.3. Comparison of Kd values with IAEA data

The IAEA TRS472 report [IAEA, 2010] presents Kd values grouped according to two criteria, namely the texture/organic matter criterion and the co-factor criterion. For the present study, comparisons of Kd values for Co, Cs and Sr are made according to the texture/organic matter criterion (Table 6.5), a classification on the basis of four main soil groups, namely sand, loam, clay and organic, defined according to the mineral matter (sand and clay mineral percentages) and organic matter content in the soil. Figure 6.9 shows a comparison of Kd values for the LFLS soils with the IAEA TRS472 dataset (Table 6.5) and the historical data set [Isaac and Mears, 1977].

Table 6.5: IAEA Kd values for Cs, Co and Sr in soils grouped according to the texture/organic matter criterion (L kg⁻¹) (reproduced from IAEA TRS472, 2010)

Element	Soil Group	N	Mean	GSD*	Minimum	Maximum
Cs	All soils	469	1200	7.0	4.3	380 000
	Sand	114	530	5.8	9.6	35 000
	Loam + Clay	227	370	3.6	39	380 000
	Organic	108	270	6.8	4.3	95 000
Co	All soils	118	480	16	2.0	100 000
	Sand + loam	89	640	16	2.0	100 000
	Clay	10	3 800	5.7	540	99 000
	Organic	17	87	9.5	4.0	5 800
Sr	All soils	255	52	5.9	0.4	6 500
	Sand	65	22	6.4	0.4	2 400
	Loam + clay	176	69	5.4	2.0	6 500

*GSD: Geometric standard deviation

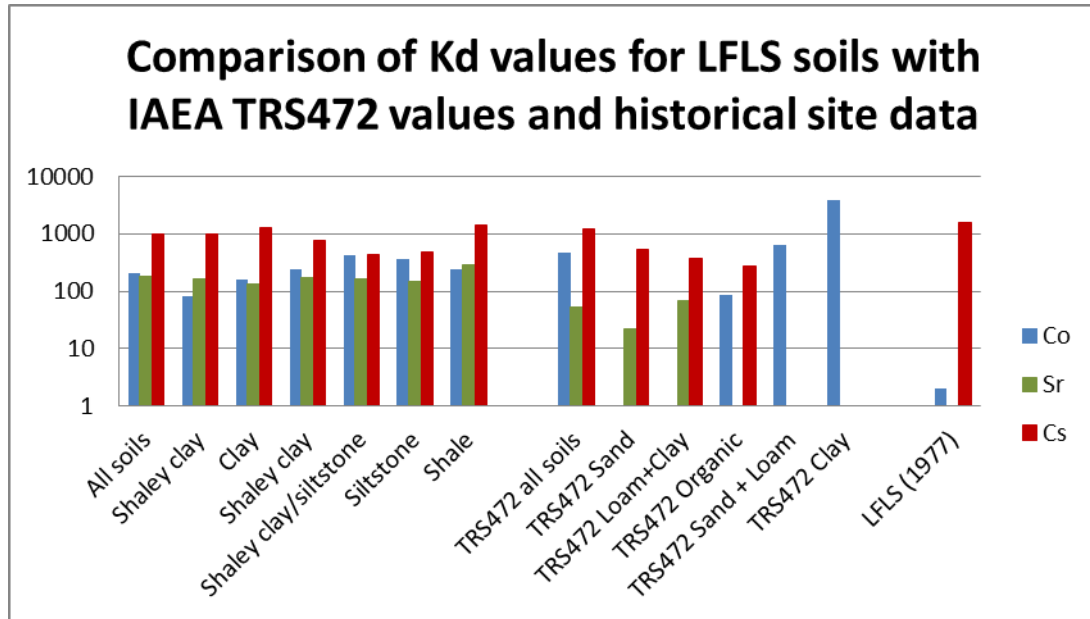


Figure 6.9: Comparison of Kd values for Co, Cs and Sr for LFLS soil material obtained in the present study with IAEA TRS472 data and LFLS historical data.

6.4. Recommended Kd values for LFLS modelling

Table 6.6 summarises the LFLS site specific Kd values for Co, Cs and Sr recommended for utilisation in various models such as groundwater fate and transport models or dose assessment models. The average Kd values reported in the Table include both the arithmetic mean (AM) and the geometric mean (GM) values from datasets representing the main lithologies at LFLS, excluding the topsoil/fill and deeper samples (> 5 m W2D samples). The geometric mean indicates the central tendency or typical value of a set of numbers by using the product of their values (as opposed to the arithmetic mean which uses their sum), bearing in mind that the Kds may be dependent on a range of (site) factors such as pH, heterogeneity of samples, particle size distribution, etc. It was also noted that where sorption was found to be > 97.5% for the radiotracer, this was not included in the sample set used to arrive at an estimated average Kd value. The justification for this was the anticipated higher (experimental) uncertainties associated with the measurement of very low solution concentrations. Therefore, an upper bound of Kd of ca 4000 L/kg was set when determining the average Kd values. However, the maximum Kd value obtained when considering the entire sample set (i.e. including sorption > 97.5%), has been provided in Table 6.6 to allow for sensitivity analysis

Table 6.6: Recommended dataset of Kd values for Co, Cs and Sr for Dose modelling of LFLS

Radionuclide	Estimated average Kd value for LFLS soils (L/kg)		Range of Kd values based on < 97.5% sorption (L/kg)	Maximum Kd noted* (L/kg)
	AM	GM		
Cs-137	1300	1000	Min-max = (310 – 4100)	4800
Sr-90	310	180	Min – max = (11 – 2300)	2300
Co-60	450	210	Min-max = (18 – 3300)	66 000

*sorption > 97.5%; AM = arithmetic mean values; GM = geometric mean values

The K_d values were estimated from batch sorption experiments for an ionic strength of 0.01 M (NaCl). The groundwater in the vicinity of the trenches at LFLS is of the Na-Cl type [Cendon et al., 2015]. The pH range considered was pH 4 to 8 with an average pH value of 5.4 ± 1.2 . This average pH value is consistent with the reported pH of groundwater across site which varies between 3.9 and 8.0 with an average of 5.4 ± 0.7 [Cendon et al., 2015]. A similar pH range was observed for borewater samples in the study of the LF site by Isaac and Mears (1977). Samples were obtained from three core holes, namely CH30, CH1A, and W2D sourced from various locations at the LFLS site to provide a range of materials representative of the site, both in the vicinity and well away from the legacy trench.

7. Sorption of Co on model minerals and simulated soil

7.1. Rationale

The purpose of the study was to delineate the key minerals present in LFLS soils that may influence the sorption of Co. A study of Cs and Sr sorption on a simulated LFLS soil and its component model minerals is reported elsewhere [Bots et al., 2019, Bots et al. 2021].

7.2. Materials and methods

7.2.1. Preparation of model soil

The simulated soil comprised the following mineral components: quartz 45%, kaolinite 25%, illite-smectite 25%, goethite 3%, anatase 2%.

7.2.2. Characterisation of model minerals.

BET surface area and CEC determinations were made of the simulated soils and various mineral components as described in Section 4.1.

7.2.3. Methodology for sorption studies

Sorption experiments were performed on the component minerals and simulated soils using a Co-57 tracer as per the method outlined in Section 5.2. K_d values were estimated from the sorption curves.

7.3. Results and Discussion

7.3.1. Geochemical characterisation of model minerals and simulated soil

Table 7.1: BET surface areas and cation exchange capacities for simulated LFLS soil and component minerals

Sample description	BET surface area, m ² /g	CEC (cmol kg ⁻¹)
Simulated soil	8.72	6.5, 6.4
Illite-smectite	29.2	26.7, 25.5
Goethite	11.8	nd
Kaolinite	8.62	4.7, 3.7
Anatase	10.5	nd
Quartz	0	nd

nd = not determined

The measured BET surface area for the simulated soil is similar to the weighted average BET value calculated from the component minerals (10 m²g⁻¹) and is dominated by the illite-smectite component

mineral. The CEC of the simulated soil is significantly lower than that for the illite-smectite component, and comparable to the CEC for the kaolinite component.

7.3.2. Sorption of Co on model minerals and simulated soil

The sorption curves for sorption of Co onto the various soil components and the LFLS simulated soil and the respective K_d values are shown in Figures 7.1 and 7.2, respectively.

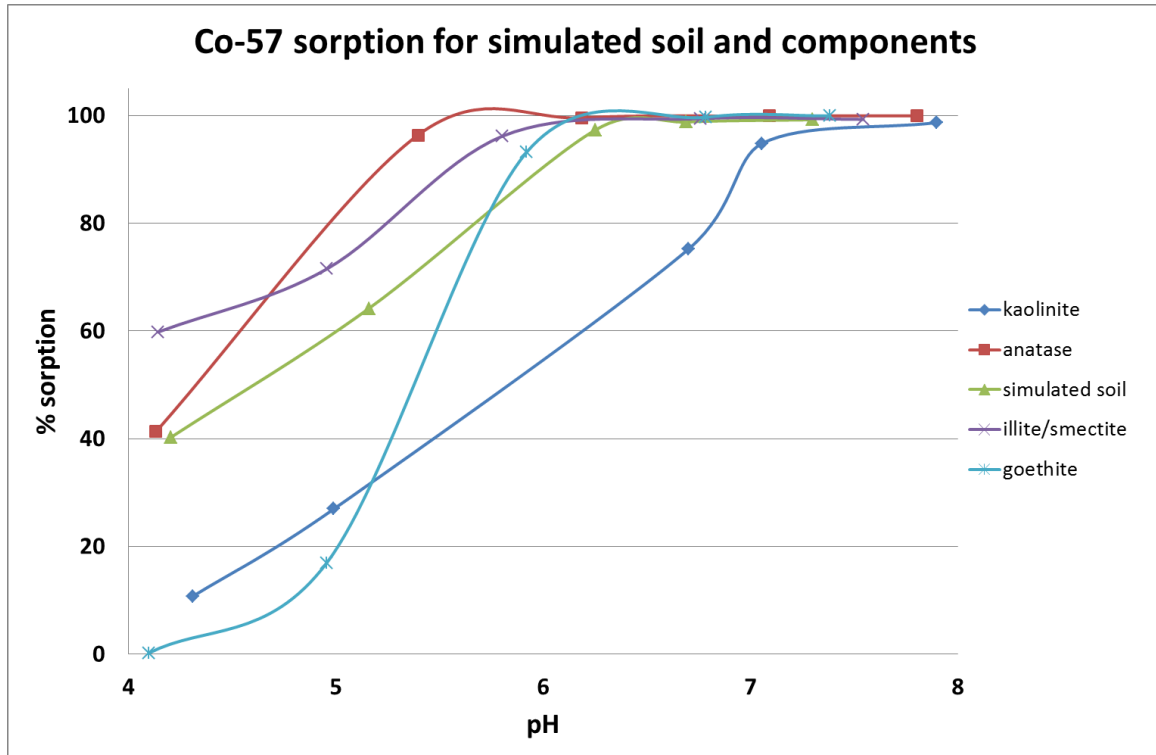


Figure 7.1: Sorption curves for sorption of Co onto LFLS simulated soil and model mineral components as a function of pH. Mass loading of 10 g/L; ionic strength 0.01 M; air equilibration; T = 25°C.

For the model component minerals, the results show that at *ca.* pH 4, both anatase and illite/smectite are the stronger sorbents relative to goethite and kaolinite, with 40% and 60% sorption of Co, respectively. At this pH, there is less than 10% sorption by kaolinite and no sorption by goethite. At pH 5, all the major soil components show at least 20% sorption, with the maximum sorption of *ca.* 80% by anatase. Anatase shows *ca.* 100% sorption at pH 5.5, whereas this occurs at pH > 6 for illite/smectite and goethite. For kaolinite, > 95% sorption occurs at pH > 7. The sorption curve of Co for the simulated soil closely mimics the sorption curve for illite/smectite which suggests that the mobility of Co is governed primarily by the illite-smectite phase through surface complexation or ion exchange. However, the small amount of anatase present in the simulated soil may also influence the mobility of Co due to the strong sorption capacity shown by this component.

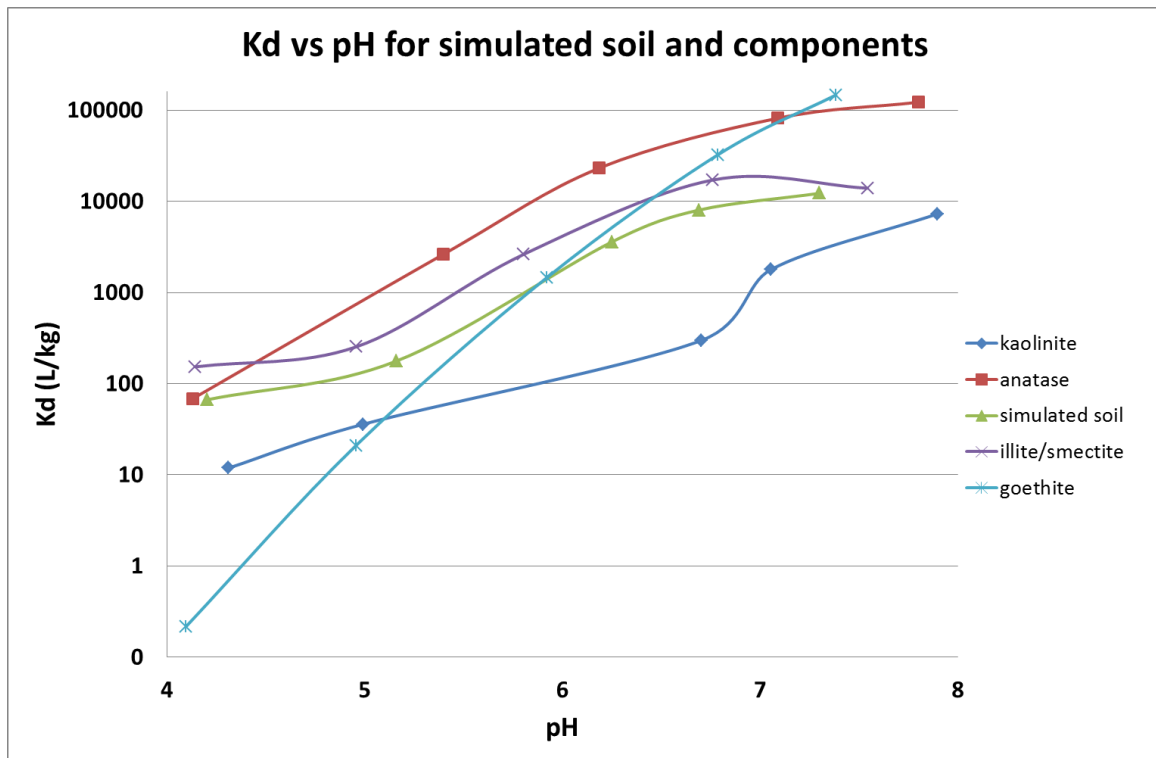


Figure 7.2: Kd for Co vs pH for LFLS model mineral and component minerals. Mass loading of 10 g/L; Ionic strength 0.01 M; air equilibration; T = 25°C.

8. Conclusions and Recommendations

The sorption of Co, Cs and Sr onto mineralogical samples taken from soil cores at the Little Forest Legacy site was investigated for a range of pH values and two ionic strengths. Samples were classed into lithological units, namely topsoil, clay, shaley clay, siltstone and shale.

Strong sorption was observed for Cs over the entire pH range, whereas the sorption of Co and Sr on the soils was found to be pH dependent.

The mobility of Cs is not significantly affected by an increase in ionic strength. The sorption of Sr was significantly reduced at the higher ionic strength over the pH range 4 to 8. The sorption of Co was significantly reduced at the higher ionic strength below pH 6. This has implications for any long term management options which lead to high salinity and/or low pH environments, particularly for the mobility of Co and Sr.

The sorption data was used to produce estimates of distribution coefficient (K_d) values for Co, Sr and Cs under controlled experimental conditions that could be utilised for various site relevant models such as groundwater fate and transport models and/or dose assessment models. Average K_d values for various lithologies and for all soils were determined.

The studies indicate limited mobility of Cs at the LFLS site which is not influenced by changes in pH, nor significantly affected by ionic strength.

At low ionic strength, K_d values for Cs sorption were similar for the majority of soils over the entire pH range, with variations of less than one order of magnitude in K_d values between samples. However, the K_d values for Sr and Co sorption were significantly lower, and varied over several orders of magnitude. K_d values were found to increase with increasing pH values, indicating a decrease in migration rate for Sr and Co with pH.

Model minerals studies for Co sorption indicate that sorption is predominantly controlled by illite/smectite and anatase.

9. Acknowledgements

We acknowledge the contributions from the following ANSTO personnel who participated in fieldwork, sample preparation, laboratory testwork, radiochemical and chemical analyses, soil property measurements, XRD analysis, data analysis, and/or scientific discussions: Dioni Cendon, Eve Chong, Matt Dore, Stuart Hankin, Mat Johansen, Inna Karatchevska, Julia Martinello, Lida Mokhber-Shahin, Brett Rowling, Pichamon Sarakan, Adella Silitonga, Sangeeth Thiruvoth, Chris Vardanega, Kerry Wilsher and Henri Wong as well as contributions from Vinzenz Brendler and Katharina Gückel from HZDR, Germany and Pieter Bots from Strathclyde University, Glasgow.







10. Bibliography


- AAEC (1985). The Little Forest Burial Ground – an information paper. Environmental Science Division. Australian Atomic Energy Commission, AAEC Report DR19. 27 pp.
- Bots, P., Pedrotti, M., Renshaw, J and Lunn, R. (2019). Immobilisation and Containment of Radioactive Waste using Colloidal Silica-Based Grout at the Little Forest Legacy Site (LFLS). Final report 2019. Department of Civil and Environmental Engineering, University of Strathclyde.
- Bots, P.; Comarmond, M.J.; Payne, T.E.; Lunn, R.J.; Rizzo, L.; Schellenger, A.E.P.; and Renshaw, J.C. (2021). An EXAFS Study on Sr and Cs Speciation in Clayey Soils at Nuclear Legacy Sites. *Environmental Science: Processes & Impacts*, 23, 1101-1115. (<https://doi.org/10.1039/d1em00121c>)
- Bradd J. (2003). A report on the hydrogeology of the Little Forest Burial Ground. Australian Nuclear Science and Technology Organisation, *ANSTO Report, EM TN_01/2003*. Lucas Heights, NSW, 61 pp.
- Cendón, D.I., Hughes, C.E., Harrison, J.J., Hankin, S. I., Johansen, M.P., Payne, T.E., Wong, H.K., Rowling, B., Vine, M., Wilsher, K., Guinea, A. and Thiruvoth S. (2015) Identification of sources and processes in a lowlevel radioactive waste site adjacent to landfills: groundwater hydrogeochemistry and isotopes, *Australian Journal of Earth Sciences: An International Geoscience Journal of the Geological Society of Australia*, 62:1, 123-141, DOI:10.1080/08120099.2015.975155
- Elbeb, M. (2009). Drilling Investigation Report: Little Forest Burial Ground, Lucas Heights, NSW, CES090517-ANS-01-F. Consulting Earth Sciences, p91.
- Hankin, S. (2012). Little Forest Burial Ground - Geology, Geophysics and Well Installation 2009–2010; *ANSTO/E-781*; Australian Nuclear Science and Technology Organisation.
- Hughes, C.E., Cendon, D.I., Harrison, J.J., Hankin, S.I., Johansen, M.P., Payne, T.E., Vine, M., Collins, R.N., Hoffmann, E.L., Loosz, T. (2011). Movement of a tritium plume in shallow groundwater at a legacy low-level radioactive waste disposal site in eastern Australia. *J. Environ. Radioact.*, 102, 943-952.
- International Atomic Energy Agency (2010). Handbook of parameter values for the prediction of radionuclide transfer in terrestrial and freshwater environments. Technical Reports Series ISSN 0074-1914; No 472, Vienna. ISBN 92-0-113009-9.
- IUPAC (1985) Reporting Physisorption data for gas/solid systems with special reference to the determination of surface area and porosity. *Pure and Applied Chemistry*, 57(4), 603-619.
- Isaacs S. R. & Mears K. F. (1977). A study of the burial ground used for radioactive waste at the Little Forest area near Lucas Heights New South Wales. Australian Atomic Energy Commission, *AAEC Report E427*, Lucas Heights, NSW, 50 pp.
- Krauskopf, K.B., (1983).. Introduction to Geochemistry. McGraw-Hill.
- Malvern Instruments Ltd. (2007). Mastersizer 2000 User Manual, MAN0384 Issue 1.0, March 2007.
- Payne, T.E., (2012). Background Report on the Little Forest Burial Ground Legacy Waste Site. *ANSTO/E-780*, ANSTO, pp. 1-23.
- Payne, T.E.; Harrison, J.J.; Hughes, C.E.; Johansen, M.P.; Thiruvoth, S.; Wilsher, K.L.; Cendón, D.I.; Hankin, S.I.; Rowling, B.; and Zawadzki, A. (2013). Trench ‘Bathtubbing’ and Surface Plutonium Contamination at a Legacy Radioactive Waste Site. *Environmental Science & Technology*, 47, 13284-13293. dx.doi.org/10.1021/es403278r.
- Payne, T.E., (2015). Little Forest Legacy Site – Summary of site history until the commencement of waste disposal in 1960. *ANSTO/E-782*, ANSTO, pp. 1-26.
- Raven, M. D. & Self P. G. (2011). XRD report—Bulk and clay fraction analysis of soil samples for ANSTO. *CSIRO Land and Water XRD Report D2381*, 25 pp, Adelaide, Australia.
- Temple R. B. & Smith E. A. J. (1959). Total cation-exchange capacities of soils from the Woronora River and the Little Forest area of Lucas Heights. Australian Atomic Energy Commission, *AAEC Report TM39*, 7 pp. Lucas Heights NSW






Rudnick, R.L & Gao, S. Composition of the Continental Crust in *Treatise on Geochemistry*, 2nd Edition (2014), Chapter 4.1, pp. 1-51. (<http://dx.doi.org/10.1016/B978-0-08-095975-7.00301-6>)

Wu, E. (2010). Groundwater monitoring well installation Little Forest Burial Ground, Lucas Heights, NSW. *Australian Nuclear Science and Technology Organisation. Coffey Environments Australia Pty Ltd*, p.23.






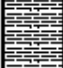
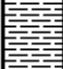
Appendix 1: Core Logs of CH1, CH1A, CH30 and W2D

Project ID: CES090517-ANS		Easting: 6231951.139		 <p>CONSULTING EARTH SCIENTISTS</p> <p><small>Jones Bay Wharf 19-21, Lower Level Suite 121 26-32 Pirrama Road Pyrmont 2009 PH: (02) 8589 2200 FAX: (02) 9552 4399</small></p>				
Project: Drilling Investigation		Northing: 313253.421						
Client: ANSTO		Elevation:						
Location: ANSTO - Little Forest Burial Ground		Environmental Log: CH1						
DRILLING INFO.			LITHOLOGY		SAMPLING INFORMATION			WELL DETAIL
Depth	Method	Water	Symbol	Description	Sample ID	Type	FID/PID (ppm) 250 500 750	
0	Direct Push			TOPSOIL: Silty clay topsoil, brown with rootlets. Moist.				
				SILTY CLAY: Brown, moist. Ironstone gravels, trace fine to medium sand and gravels.				
				CLAY: Brown/orange with red colourations, medium to high plasticity, moist, no odour. Ironstone gravels, trace fine to medium gravels.				
				SHALEY CLAY: Orange/brown with ironstone gravels. Dry.				
				SHALE: Extremely weathered Shale with siltstone bandings. Light brown and dry. Due to rock formation, sample tube missing from 2 m to 3 m. Push tube refusal @ 3.00 m.				
3				End of corehole. Corehole terminated at 3.00 m (practical refusal).				
4								
5								
Drill Company: Macquarie Drilling		Date Commenced: 04/08/2009						
Drill Model: Geoprobe 7720DT		Date Completed: 04/08/2009						
Hole Diameter (mm): 83		Logged/checked by: M Elbeb						
				Sheet: 1 of 1				

Project ID: CES090517-ANS	Easting: 313253.958	 <p>CONSULTING EARTH SCIENTISTS <small>Jones Bay Wharf 19-21, Lower Level Suite 121 26-32 Pirrama Road Pyrmont 2009 PH: (02) 8569 2200 FAX: (02) 9552 4399</small></p>
Project: Drilling Investigation	Northing: 6231951.311	
Client: ANSTO	Elevation:	
Location: ANSTO - Little Forest Burial Ground	Environmental Log: CH1A	

DRILLING INFO.			LITHOLOGY		SAMPLING INFORMATION				WELL DETAIL			
Depth	Method	Water	Symbol	Description	Sample ID	Type	FID/PID (ppm)					
							0	250	500	750		
0	↑ Direct Push ↓			TOPSOIL: Silty clay topsoil, brown with rootlets. Moist.							0	
1				SILTY CLAY: Brown, moist. Ironstone gravels, trace fine to medium sand and gravels.							1	
2				CLAY: Brown/orange with red colourations, medium to high plasticity, moist, no odour. Ironstone gravels, trace fine to medium gravels.								2
3				SHALEY CLAY: Orange/brown with ironstone gravels. Dry.								3
4				SHALE: Extremely weathered Shale with siltstone bandings. Light brown becoming brown with depth. Dry. Push tube refusal @ 4.00m.								4
5				End of corehole. Corehole terminated at 4.00 m (practical refusal).							5	

Drill Company: Macquarie Drilling	Date Commenced: 04/08/2009
Drill Model: Geoprobe 7720DT	Date Completed: 04/08/2009
Hole Diameter (mm): 83	Logged/checked by: M Elbeb
Sheet: 1 of 1	

Project ID: CES090517-ANS		Easting: 313265.553		 <p>Jones Bay Wharf 19-21, Lower Level Suite 121 28-32 Pirrama Road Pyrmont 2009 PH: (02) 8569 2200 FAX: (02) 9552 4399</p>					
Project: Drilling Investigation		Northing: 6231967.183							
Client: ANSTO		Elevation:							
Location: ANSTO - Little Forest Burial Ground		Environmental Log: CH30							
DRILLING INFO.			LITHOLOGY		SAMPLING INFORMATION			WELL DETAIL	
Depth	Method	Water	Symbol	Description	Sample ID	Type	FID/PID (ppm)		
							250 500 750		
0	Direct Push			FILL: Brown, moist. Black charcoal inclusion. Ironstone gravels, trace fine to medium sand and gravels.					
					SILTY CLAY: Dark brown, moist. Black charcoal inclusion. Ironstone gravels, trace fine to medium sand and gravels.				
1				CLAY: Brown/orange with red colourations. Black charcoal inclusions throughout, medium to high plasticity, moist. Ironstone gravels throughout, trace fine to medium gravels.					
				SHALEY CLAY: Orange/brown colourations, ironstone gravels, trace fine to medium gravels. Dry.					
2				SILTSTONE: Extremely weathered siltstone with shale bandings. Light brown/grey becoming brown with depth. Dry. Push tube refusal @ 2.00 m.					
	SFA			SHALE: Extremely weathered Shale with siltstone bandings. Light brown/grey with depth. Wet from 4.5 m.					
3									
4									
5				End of corehole. Corehole terminated at 5.00 m (limit of investigation).					
Drill Company: Macquarie Drilling		Date Commenced: 05/08/2009		Drill Model: Geoprobe 7720DT		Date Completed: 05/08/2009		Hole Diameter (mm): 83	
		Logged/checked by: M Elbeb						Sheet: 1 of 1	



Environmental Log - Piezometer

Client: **ANSTO**
 Principal:
 Project: **Little Forest Burial Ground, Groundwater Assessment**
 Borehole Location: **Little Forest Burial Ground, Lucas Hts.**

Borehole No. **W2d**
 Sheet 1 of 3
 Office Job No.: **ENAU RHOD04037AA**
 Date started: **20.9.2010**
 Date completed: **23.9.2010**
 Logged by: **NC**
 Checked by: **EW**

drilling information		material substance								
method	penetration	notes samples, tests, etc.	well details	RL	depth metres	graphic exp classification symbol	material	moisture cond lon	consistency/density index	structure and additional observations
1 2 3	support water						soil type: plasticity or particle characteristics, colour, secondary and minor components.			
ADT (100mm)					1.00	SM	Topsoil: Silty SAND: Fine grained, brown to dark brown. Traces of rootlets. Traces of fine ironstone gravel, red brown.	M	L	Grass on surface
					1.10	CH	Silty CLAY: Low to medium plasticity, red brown.	<Wp	F	
					1.20	DH	CLAY: Low to medium plasticity, red brown with grey (extremely weathered shale)	<Wp	F-SI	
					1.30		SHALE: Extremely weathered, very low strength, grey to pale brown. Some clay banding.	D		
					1.25		SHALE: Extremely weathered, very low strength, grey to pale brown. Clay bandings, red brown ironstone staining.	D		
					1.20		CLAY: Low to medium plasticity, brown to pale brown with red brown. Shale banding, grey, indistinct. Traces of silt.	<Wp	F-SI	
					1.10		SHALE: Extremely weathered, low strength, grey to dark grey, minor pale brown. Some clay banding.	M		
					1.07		Sandy SILTSTONE: Very low strength grey. Sandy bands, very fine grained, some quartz.	D		
					1.05		SHALE: Moderate strength, dark grey, distinct. Some brown colour banding. Becoming moist.	M		
					1.00					
					1.20					

PIEZOMETER ENAU RHOD04037AAJ-DSS GPJ COFFEY DDT 28.10.10

Form (REV. 5.9) (Rev. 3 Rev. 4)

method AS auger screwing* AC auger drilling* NN roller/drone W washbore CT cable tool DT derrick B bank bit V V bit T TC bit TBX Tubes *bit shown by suffix #GP	support C casing N nit penetration 1 2 3 4 no resistance reaching to refusal water 10/101 water level on date shown water inflow water outflow	notes, samples, tests U ₂₀ undisturbed sample 50mm diameter D disturbed sample N standard penetration test (SPT) N* SPT - sample recovered No SPT with solid cone P pressure meter B bulk sample R refusal E environmental sample FID FID measurement WS water sample P2 piezometer ALT air lift test	moisture D dry M moist W wet Wp plastic limit W _L liquid limit	consistency/density index VE very soft S soft F firm SI stiff VSI very stiff H hard Rb friable VL very loose L loose MD medium dense D dense VD very dense
------------------------------------------------------------------------------------------------------------------------------------------------------------------------------------------------------------	--------------------------------------------------------------------------------------------------------------------------------------------------------------------------------------	----------------------------------------------------------------------------------------------------------------------------------------------------------------------------------------------------------------------------------------------------------------------------------------------------------------------------------------------------------------	-------------------------------------------------------------------------------------------------	-------------------------------------------------------------------------------------------------------------------------------------------------------------------------------------------------------



Environmental Log - Piezometer

Client: **ANSTO**

Principal:

Project: **Little Forest Burial Ground, Groundwater Assessment**

Borehole Location: **Little Forest Burial Ground, Lucas Hts.**

Borehole No. **W2d**

Sheet 2 of 3

Office Job No.: **ENAU RHOD04037AA**

Date started: **20.9.2010**

Date completed: **23.9.2010**

Logged by: **NC**

Checked by: **EW**

drill model & mounting: Edson MRA260 Ute	Easting: 313169.9	slope: -90°	R.L. Surface: 132.88
hole diameter: 150/95	Northing: 6231833.7	bearing:	datum: AHD

drilling information				material substance			
method	penetration	support	notes samples, tests, etc	well details	depth metres	material	structure and additional observations
1 2 3				RL		soil type: plasticity or particle characteristics, colour, secondary and minor components.	
AS		C casing			11	SHALE: Moderate strength, dark grey. Distinct. Some brown colour banding. (continued)	
AD					12	Saturated	
RR					13		
W					14		
CT					15		
DT					16	SANDSTONE: Medium grained, grey to orange.	
B					17		Rapid Groundwater inflow into open borehole.
V					18		
T					19		
TBX					20	Orange colouring decreasing, predominantly grey.	
							Hawkesbury Sandstone. Difficult to establish moisture due to upper aquifer.

PIEZOMETER ENAU RHOD04037AA-LOGS.GPJ COFFEY.GDT 28.10.10

method AS auger screwing* AD auger drilling* RR roller/tricone W washbore CT cable tool DT diatube B blank bit V V bit T TC bit TBX Tubex *bit shown by suffix e.g. ADT	support C casing N nil penetration 1 2 3 4 1 no resistance ranging to refusal 2 3 4 water 10/1/98 water level on date shown water inflow water outflow	notes, samples, tests U ₅₀ undisturbed sample 50mm diameter D disturbed sample N standard penetration test (SPT) N* SPT - sample recovered Nc SPT with solid cone P pressure meter Bs bulk sample R refusal E environmental sample PID PID measurement WS water sample PZ piezometer ALT air lift test	moisture D dry M moist W wet Wp plastic limit W _L liquid limit	consistency/density index VS very soft S soft F firm St stiff VSt very stiff H hard Fb friable VL very loose L loose MD medium dense D dense VD very dense
--------------------------------------------------------------------------------------------------------------------------------------------------------------------------------------------------------------------	-----------------------------------------------------------------------------------------------------------------------------------------------------------------------------------------------------------------	-----------------------------------------------------------------------------------------------------------------------------------------------------------------------------------------------------------------------------------------------------------------------------------------------------------------------------------------------------------------	-------------------------------------------------------------------------------------------------	-------------------------------------------------------------------------------------------------------------------------------------------------------------------------------------------------------

Appendix 2: Compilation of sorption data and Kd data for LFLS soils

Sorption of Co, Sr and Cs at 0.01 M ionic strength. Experimental conditions 0.01M

Corehole	Depth (cm)	Lithology	Target pH	Final pH	% Co-57 sorbed	% Sr-85 sorbed	% Cs-137 sorbed	Kd Co-57 (mL/g)	Kd Sr-85 (mL/g)	Kd Cs-137 (mL/g)
CH1	0- 20	Topsoil	4.5	4.67	49%	33%	86%	96	48	595
CH1	0- 20	Topsoil	5.5	5.39	80%	58%	90%	406	137	943
CH1	0- 20	Topsoil	6.5	6.89	95%	83%	93%	1725	496	1235
CH1A	40-60	clay	3	3.16		7.2	94.4		7	1500
CH1A	40-60	clay	4	4.13		25.3	96.6		33	2768
CH1A	40-60	clay	5	4.89		66.1	98.0		192	4819
CH1A	40-60	clay	6	5.80		78.8	95.5		364	2099
CH1A	40-60	clay	7	6.85		76.7	93.2		323	1344
CH1A	40-60	clay	8	7.40		88.9	96.5		776	2662
CH1A	40-60	clay	3	3.05	4.0			4		
CH1A	40-60	clay	4	3.98	16.4			18		
CH1A	40-60	clay	5	4.99	54.7			117		
CH1A	40-60	clay	6	5.95	83.7			487		
CH1A	40-60	clay	7	7.04	98.1			5106		
CH1A	40-60	clay	8	8.04	97.8			4312		
CH1A	40-60	clay	9	8.96	90.7			957		
CH1A	40-60	clay	3	3.05	3.8			4		
CH1A	140-160	shaley clay	3	3.06		15.6	92.5		18	1194
CH1A	140-160	shaley clay	4	4.07		49.7	94.9		97	1835
CH1A	140-160	shaley clay	5	4.85		75.1	94.6		293	1716
CH1A	140-160	shaley clay	6	5.64		90.3	94.3		891	1591
CH1A	140-160	shaley clay	7	6.64		83.6	88.6		498	759
CH1A	140-160	shaley clay	8	7.52		86.5	89.1		635	809
CH1A	140-160	shaley clay	3.0	3.01	16.6			18		
CH1A	140-160	shaley clay	4.0	4.02	35.6			53		
CH1A	140-160	shaley clay	5.0	4.91	76.6			307		
CH1A	140-160	shaley clay	6.0	5.70	91.9			1118		
CH1A	140-160	shaley clay	7.0	6.76	99.4			17485		
CH1A	140-160	shaley clay	8.0	7.78	99.4			15772		
CH1A	140-160	shaley clay	9.0	8.88	96.0			2364		
CH1A	140-160	shaley clay	4.5	4.38	47.5			88		
CH1A	140-160	shaley clay	5.5	5.39	82.9			466		
CH1A	140-160	shaley clay	4.3	4.41	61.9	61.7	96.4	163	162	2653
CH1A	240-260	shale	3	3.11		17.5	89.5		21	822
CH1A	240-260	shale	4	4.08		48.9	93.1		92	1308
CH1A	240-260	shale	5	4.85		56.1	85.5		125	579
CH1A	240-260	shale	6	5.74		82.6	88.7		462	769
CH1A	240-260	shale	7	6.92		89.1	89.7		790	838
CH1A	240-260	shale	8	7.55		87.8	85.8		710	594
CH1A	240-260	shale	3	3.05	14.9			17		
CH1A	240-260	shale	4	4.02	33.4			50		
CH1A	240-260	shale	5	4.93	68.8			218		
CH1A	240-260	shale	6	5.78	88.1			722		
CH1A	240-260	shale	7	6.79	97.1			3283		
CH1A	240-260	shale	8	7.72	97.7			4157		
CH1A	240-260	shale	9	9.00	82.7			474		
CH1A	240-260	shale	4.5	4.58	53.6			115		
CH1A	240-260	shale	5.5	5.32	64.4			179		
CH1A	340-360	shale	3	3.05		18.2	95.3		22	2022
CH1A	340-360	shale	4	4.03		49.4	97.4		96	3605
CH1A	340-360	shale	5	4.94		79.8	97.8		396	4534
CH1A	340-360	shale	6	5.89		92.1	97.6		1145	3974
CH1A	340-360	shale	7	6.80		93.8	97.1		1510	3377
CH1A	340-360	shale	8	7.50		95.8	97.3		2252	3582
CH1A	340-360	shale	3	2.99	10.9			12		
CH1A	340-360	shale	4	3.98	37.8			60		
CH1A	340-360	shale	5	4.96	67.0			198		
CH1A	340-360	shale	6	5.86	87.3			675		
CH1A	340-360	shale	7	7.03	98.9			8923		
CH1A	340-360	shale	8	7.97	96.5			2774		
CH1A	340-360	shale	9	8.97	78.9			366		
CH1A	340-360	shale	4.5	4.52	54.5			120		
CH1A	340-360	shale	5.5	5.36	74.1			283		

Corehole	Depth (cm)	Description	Target pH	Final pH	% Co-57 sorbed	% Sr-85 sorbed	% Cs-137 sorbed	Kd Co-57 (mL/g)	Kd Sr-85 (mL/g)	Kd Cs-137 (mL/g)
CH30	0-20	Fill	4.5	4.91	42%	42%	78%	72	72	356
CH30	0-20	Fill	4.5	4.56	41%	51%	91%	62	92	852
CH30	0-20	Fill	5.5	7.03	57%	53%	91%	134	111	962
CH30	0-20	Fill	5.5	4.93	93%	53%	93%	180	110	1260
CH30	0-20	Fill	5.5	5.52	56%	50%	87%	137	107	708
CH30	0-20	Fill	6.5	6.46	96%	65%	89%	2510	213	948
CH30	20-40	Silty clay	4.5	4.73	66%	21%	91%	188	25	953
CH30	20-40	Silty clay	5.5	6.17	88%	36%	92%	744	55	1186
CH30	20-40	Silty clay	5.5	5.00	95%	34%	95%	546	50	1750
CH30	40-60	Clay	4.5	4.98	55%	47%	91%	121	88	941
CH30	40-60	Clay	5.5	6.03	89%	55%	92%	771	119	1149
CH30	40-60	Clay	5.5	4.97	94%	42%	94%	183	72	1702
CH30	60-80	Clay	4.5	4.95	55%	55%	93%	122	121	1210
CH30	60-80	Clay	5.5	6.53	51%	47%	87%	105	89	660
CH30	60-80	Clay	5.5	4.84	94%	47%	94%	174	88	1610
CH30	80-100	Clay	4.5	4.34	91%	32%	91%	123	46	1034
CH30	80-100	Clay	5.5	6.09	57%	52%	93%	129	108	1268
CH30	80-100	Clay	5.5	4.81	93%	47%	93%	172	87	1324
CH30	80-100	Clay	5.5	4.88	35%	34%	90%	52	50	841
CH30	80-100	Clay	6.5	5.99	76%	59%	93%	318	142	1376
CH30	100-120	shaley clay	4.5	4.30	83%	34%	83%	123	52	473
CH30	100-120	shaley clay	5.5	6.64	66%	61%	88%	195	157	699
CH30	100-120	shaley clay	5.5	4.98	86%	53%	86%	179	111	622
CH30	100-120	shaley clay	5.5	4.97	44%	39%	76%	77	62	311
CH30	100-120	shaley clay	6.5	6.52	97%	70%	86%	3253	234	591
CH30	120-140	shaley clay	4.5	4.29	87%	37%	87%	131	58	635
CH30	120-140	shaley clay	5.5	5.46	57%	52%	76%	131	108	315
CH30	120-140	shaley clay	6.5	6.68	93%	64%	82%	1226	173	451
CH30	140-160	shaley clay/siltstone	4.5	4.77	84%	60%	84%	212	148	517
CH30	140-160	shaley clay/siltstone	5.5	5.64	61%	53%	77%	154	112	326
CH30	140-160	shaley clay/siltstone	6.5	6.69	96%	71%	84%	2447	239	518
CH30	160-180	siltstone	4.5	4.90	83%	54%	83%	190	115	493
CH30	160-180	siltstone	5.5	5.65	61%	55%	78%	153	118	337
CH30	160-180	siltstone	6.5	6.86	94%	65%	83%	1599	182	469
CH30	180-200	siltstone	4.5	4.91	86%	61%	86%	199	151	600
CH30	180-200	siltstone	5.5	5.77	71%	58%	80%	240	138	399
CH30	180-200	siltstone	6.5	6.79	90%	68%	87%	933	206	648

Corehole	Depth (cm)	Description	Target pH	Final pH	Percentage of Co-57 (region1) in solid phase	Percentage of Sr-85 in solid phase	Percentage of Cs-137 in solid phase	Kd Co-57 (region1) (mL/g)	Kd Sr-85 (mL/g)	Kd Cs-137 (mL/g)
W2D	0- 50	Topsoil	4.5	4.46	33%	31%	85%	48	45	571
W2D	0- 50	Topsoil	5.5	4.94	45%	37%	78%	80	58	353
W2D	0- 50	Topsoil	6.5	6.81	87%	66%	86%	641	194	627
W2D	100-150	Silty clay	4	4.24	18.3	9.9	87.0	23	11	676
W2D	100-150	Silty clay	natural pH	4.32	30.2	26.7	94.2	43	36	1604
W2D	100-150	Silty clay	5	5.01	67.7	64.1	91.2	216	183	1072
W2D	100-150	Silty clay	5.5	5.37	69.7	61.4	80.8	226	156	414
W2D	100-150	Silty clay	6	6.04	98.4	87.5	91.0	6175	721	1040
W2D	100-150	Silty clay	7	6.76	99.6	89.1	91.1	24732	828	1039
W2D	100-150	Silty clay	8	7.57	99.8	90.3	91.8	65847	945	1136
W2D	100-150	Silty clay	4.4	4.57	42.5	38.5	95.5	74	63	2116
W2D	250-300	SHALE	4	4.11	16.8	11.9	88.5	21	14	797
W2D	250-300	SHALE	natural pH	4.68	45.1	41.6	93.2	82	71	1367
W2D	250-300	SHALE	natural pH	4.69	53.2	49.8	96.6	113	98	2827
W2D	250-300	SHALE	5	5.04	63.1	61.8	93.3	180	170	1461
W2D	250-300	SHALE	5.5	5.42	75.1	74.2	88.7	300	286	781
W2D	250-300	SHALE	6	6.04	93.4	81.3	90.1	1524	467	979
W2D	250-300	SHALE	7	7.05	99.1	81.2	88.8	11382	466	860
W2D	250-300	SHALE	8	7.63	99.6	86.3	91.4	27249	720	1210
W2D	250-300	SHALE	4.8	4.94	66.0	64.0	97.5	199	183	4071
W2D	450-500	CLAY	natural pH	4.86	69.8	70.2	96.2	231	236	2523
W2D	450-500	CLAY	5.5	5.43	67.4	69.6	80.4	205	226	405
W2D	450-500	CLAY	5	5.30	76.1	76.0	95.2	326	317	1979
W2D	650	SILTSTONE	natural pH	7.02	91.2	51.4	69.2	1036	106	225
W2D	950	shale	natural pH	7.13	85.6	57.8	89.0	593	137	807
W2D	1750	sandstone	natural pH	6.93	72.7	52.8	87.2	263	111	675

Sorption of Co, Sr and Cs at 0.1 M ionic strength. Experimental conditions:

Corehole	Depth (cm)	Lithology	Target pH	Final pH	% Co-57 sorbed	% Sr-85 sorbed	% Cs-137 sorbed	Kd Co-57 (mL/g)	Kd Sr-85 (mL/g)	Kd Cs-137 (mL/g)
KG11A	40-60	clay	3	3.1	5.7	7.5	91.7	6.0	8.1	1105
KG11B	40-60	clay	4	4.2	9.8	9.9	94.7	10.5	10.6	1746
KG11C	40-60	clay	5	4.9	24.9	18.2	94.5	32.5	21.8	1680
KG11D	40-60	clay	6	5.8	79.4	24.9	94.6	380	32.7	1711
KG11E	40-60	clay	7	7.0	98.2	37.0	93.9	5308	56.5	1493
KG11F	40-60	clay	8	7.7	98.4	49.2	94.3	6140	94.2	1597
KG12A	140-160	shaley clay	3	3.1	7.8	7.9	90.1	8.4	8.4	899
KG12B	140-160	shaley clay	4	4.1	9.9	11.1	93.2	10.8	12.3	1347
KG12C	140-160	shaley clay	5	4.9	18.4	18.4	91.6	22.3	22.2	1071
KG12D	140-160	shaley clay	6	5.7	80.1	24.2	92.0	393	31.1	1124
KG12E	140-160	shaley clay	7	7.1	98.9	25.2	90.2	8,769	33.1	901
KG12F	140-160	shaley clay	8	7.9	99.2	30.4	89.0	12,070	43.0	796
KG13A	240-260	shale	3	3.1	9.9	13.3	82.8	10.9	15.1	477
KG13B	240-260	shale	4	4.0	12.8	16.5	90.9	14.3	19.4	975
KG13C	240-260	shale	5	4.8	16.4	20.5	87.5	19.6	25.8	705
KG13D	240-260	shale	6	5.7	70.1	24.2	87.1	228	31.1	656
KG13E	240-260	shale	7	7.0	98.3	29.7	86.3	5480	41.2	613
KG13F	240-260	shale	8	7.9	99.0	43.9	88.0	9982	77.6	729
KG14A	340-360	shale	3	3.1	2.9	3.5	85.5	2.9	3.6	580
KG14B	340-360	shale	4	4.0	6.6	8.1	91.9	7.0	8.8	1130
KG14C	340-360	shale	5	4.9	14.6	14.3	88.8	16.5	16.1	767
KG14D	340-360	shale	6	5.9	76.3	20.9	86.5	319	26.2	635
KG14E	340-360	shale	7	7.1	98.5	41.1	86.7	6145	67.4	631
KG14F	340-360	shale	8	7.9	99.3	58.3	82.2	14272	136.2	450

End of Document